P516524.PDF [Page: 4 of 44]

Copy No. 16

DEFENCE R&D DÉFENSE

ZOOPLANKTON AGGREGATIONS NEAR A COASTAL SILL: AN EXAMINATION OF ECHO-SOUNDER DATA FROM AUGUST AND SEPTEMBER 1995 IN KNIGHT INLET, B.C.

M.V Trevorrow
DREA

Defence R&D Canada

Technical Memorandum
DREA TM 2001-119
September 2001

National Defence / Défense nationale

Canada

Zooplankton Aggregations Near a Coastal Sill: An Examination of Echo-Sounder Data from August and September 1995 in Knight Inlet, B.C.

Mark V. Trevorrow
DREA

Defence Research Establishment Atlantic

Technical Memorandum

DREA TM 2001-119

September 2001

Author

Mark V. Trevorrow

Approved by

Ron Kuwahara

Head, Electromagnetics Section

Approved for release by

Kirk Foster

Chair, DREA Document Review Panel

© Her Majesty the Queen as represented by the Minister of National Defence, 2001

© Sa majesté la reine, représentée par le ministre de la Défense nationale, 2001

Abstract

(U) This report presents a retrospective study of echo-sounder and other physical oceanographic data collected in Knight Inlet, British Columbia during the late summer of 1995. This present study was undertaken to provide oceanographic background and assist planning for focused field experiments on zooplankton aggregations which will be conducted in this same area in the autumn of 2001. High-frequency (120 and 200 kHz, uncalibrated) echo-sounder data from two separate vessels is examined under both ebb and flood tide conditions, and for diurnal variations. The 1995 data revealed dramatic tidally-driven internal hydraulic flows over-top of a 65 m deep sill in Knight Inlet, created by strong, near-surface (<20 m depth) thermohaline stratification. In general the zooplankton populations exhibited classic diurnal migration habits, forming into relatively dense layers at 70 to 120 m depth during daytime and dispersing throughout the entire water column at night. This behavior is suggestive that the zooplankton scattering layers were dominated by Euphausiids, which are common in B.C. coastal inlets. During daytime on both ebb and flood tides there was evidence that the zooplankton layers were trapped and concentrated by the flow against the upstream side of the sill. A comparison of acoustic scattering with *in situ* temperature, salinity, and turbulence profiles suggests that microstructure scattering is responsible for distinct *flow lines* appearing in the strongly stratified near-surface region, however zooplankton scattering is found to dominate at greater depths. For the autumn 2001 field experiments, behavioral hypotheses and recommendations are given for using calibrated, multi-frequency echo-sounders in conjunction with net trawls and *in situ* optical sampling techniques.

Résumé

(NC) Ce rapport présente une étude rétrospective de données d'échosondeurs et d'autres données d'océanographie physique recueillies au Knight Inlet, en Colombie Britanique, à la fin de l'été 1995. L'étude a été entreprise afin d'établir le contexte océanographique pour la planification d'expériences dirigées qui seront menées sur des agrégations de zooplancton au même endroit, à l'automne 2001. Des données d'échosondeurs à haute fréquence (120 et 200 kHz, appareils non calibrés) obtenues à partir de deux navires lors de marées montantes et descendantes, ainsi que sur des cycles diurnes, sont examinées. Les données de 1995 ont mis en évidence d'importants courants de marée internes sur un seuil d'une profondeur de 65 m dans Knight Inlet, lesquels sont créés par une forte stratification thermohaline près de la surface (profondeur < 20 m). En général, les populations de zooplancton effectuaient des migrations diurnes classiques, formant des couches relativement denses à des profondeurs variant entre 70 et 120 m pendant le jour et se dispersant dans l'ensemble de la colonne d'eau la nuit. Ce comportement laisse croire que le zooplancton formant les couches de dispersion était dominé par des euphausiacés, qui sont abondants dans les indentations de la côte de la C.-B. Les données indiquent que, durant le jour, tant lorsque la marée monte que lorsqu'elle descend, les couches de zooplancton se trouvent coincées et concentrées par le courant contre

P516524.PDF [Page: 8 of 44]

la partie en amont du seuil. La comparaison de la dispersion acoustique aux profils de température, de salinité et de turbulence laisse croire que les *lignes de flux* distinctes qui apparaissent dans la zone fortement stratifiée près de la surface sont attribuables à la dispersion microstructurale, mais la dispersion causée par le zooplancton domine à de plus grandes profondeurs. Pour l'expérience de l'automne 2001, des hypothèses liées au comportement du zooplancton et des recommandations sont présentées en vue d'utiliser des échosondeurs multifréquences calibrés de concert avec des filets à plancton et des mesures optiques *in situ*.

P516524.PDF [Page: 9 of 44]

Executive summary

Introduction
As a prelude to a focused investigation of zooplankton aggregations near coastal sills to be conducted in Knight Inlet, B.C. in the autumn of 2001, this work presents a retrospective look at echo-sounder and other oceanographic data collected in this area in the late summer of 1995. In this area, the interaction of strong near-surface stratification with tidally-driven flows over a relatively shallow sill creates dramatic internal hydraulic flows. It is hypothesized that zooplankton communities will be strongly influenced by these flows, for example by concentration within zones of flow convergence, and will exhibit significant behavioural responses, such as sinking in the presence of turbulence.

Principal Results
The uncalibrated, high-frequency echo-sounders produced high-resolution images of zooplankton populations within the context of flow in and around the sill at Knight Inlet. The zooplankton populations exhibited classic diurnal migrations habits, forming into relatively dense layers at 70 to 120 m depth during daytime and dispersing throughout the entire water column at night. During daytime on both ebb and flood tides there was evidence that the zooplankton layers were trapped and concentrated by the flow against the upstream side of the sill. A comparison of acoustic scattering with *in situ* temperature, salinity, and turbulence profiles suggested that microstructure scattering was responsible for distinct *flow lines* appearing in the strongly stratified near-surface region, however zooplankton scattering was found to dominate at greater depths.

Significance of the Results
The 1995 data provides a physical oceanographic context and gives some preliminary ideas about zooplankton distributions that will prove invaluable in designing survey strategies in future sea trials. Shortcomings of this data have highlighted the need for a combined bio-acoustic approach using multi-frequency calibrated echo-sounders, zooplankton tows, and *in situ* orientation and behavioural measurements.

Future Plans
A focused field survey on zooplankton aggregations near this Knight Inlet sill will be conducted by a combined team, including the author and scientists from the Institute of Ocean Sciences (Fisheries & Oceans, Sidney, BC) and Louisiana State University. This field survey will be performed on board the CCGS Vector in November, 2001. Follow-on experiments in 2002 are contemplated.

Trevorrow, Mark V. 2001. Zooplankton Aggregations Near a Coastal Sill: An Examination of Echo-Sounder Data from August and September 1995 in Knight Inlet, B.C. TM 2001-119. DREA.

?516524.PDF [Page: 10 of 44]

Sommaire

Introduction
Pour préparer une investigation dirigée des agrégations de zooplancton à proximité des seuils côtiers qui sera menée à l'automne 2001, au Knight Inlet en Colombie Britannique, cette étude examine rétrospectivement des données acoustiques et d'autres données océanographiques recueillies à cet endroit à la fin de l'été 1995. Dans cette region, l'interaction entre une forte stratification près de la surface et des courants de marée au-dessus d'un seuil relativement peu profond engendre d'importants courants internes. On pose l'hypothèse selon laquelle ces courants influent fortement sur les communautés de zooplancton (par exemple, les organismes seraient concentrés dans les zones de convergence des courants) et que le zooplancton présente d'importantes réactions comportementales, comme se laisser descendre dans la colonne d'eau lorsqu'il y a turbulence.

Principaux resultants
Les échosondeurs à haute fréquence non calibrés ont produit des images à haute résolution de populations de zooplancton dans le contexte des mouvements d'eau près du seuil dans le Knight Inlet. Les populations de zooplancton effectuaient des migrations diurnes classiques, formant des couches relativement denses à des profondeurs variant entre 70 et 120 m pendant le jour et se dispersant dans l'ensemble de la colonne d'eau la nuit. Les données indiquent que, durant le jour, tant lorsque la marée monte que lorsqu'elle descend, les couches de zooplancton se trouvent coincées et concentrées par le courant contre la partie en amont du seuil. La comparaison de la dispersion acoustique aux profils de température, de salinité et de turbulence laisse croire que les *lignes de flux* distinctes qui apparaissent dans la zone fortement stratifiée près de la surface sont attribuables à la dispersion microstructurale, mais la dispersion causée par le zooplancton domine à de plus grandes profondeurs.

Portée des resultants
Les données de 1995 établissent le contexte physique du milieu marin et donnent des idées préliminaires sur la répartition du zooplancton qui s'avéreront utiles à la conception de stratégies de relevé pour de futurs essais en mer. Les lacunes dans ces données ont mis en évidence le besoin d'adopter une démarche bio-acoustique qui combine l'utilisation d'échosondeurs multifréquences calibrés, l'échantillonnage du zooplancton et des mesures *in situ* de l'orientation et du comportement du zooplancton.

Suivi
Une équipe formée de l'auteur et de scientifiques de l'Institut des sciences de la mer (Pêches et Océans, Sidney, C.-B.) et de la Louisiana State University réalisera une étude dirigée des agrégations de zooplancton près du seuil dans le Knight Inlet. L'étude sera effectuée à bord du NGCC Vector en novembre 2001. On envisage de réaliser des expériences de suivi en 2002.

Trevorrow, Mark V. 2001. Zooplankton Aggregations Near a Coastal Sill: An Examination of Echo-Sounder Data from August and September 1995 in Knight Inlet, B.C. TM 2001-119. DREA.

P516524.PDF [Page: 11 of 44]

Acknowledgments

The analysis work performed by the author and reported herein was supported by an award from the U.S. Office of Naval Research (Dr. J. Eckman, Code 322BC). The author is grateful for this support and the continuing support for field trials in 2001 and 2002. The original 1995 Knight Inlet experiments were supported by grants from US ONR (Dr. L. Goodman) to Dr. David Farmer and others. CTD and echo-sounder data from the *CSS Vector* was provided courtesy of Dr. David Farmer at the Institute of Ocean Sciences. The assistance of Grace Kamitakahara at IOS in retrieving the echo-sounder and CTD data is greatly appreciated. Tide gauge, echo-sounder, and Advanced Microstructure Profiler data from the *RV Miller* were provided courtesy of Drs. Mike Gregg and Jody Klymak of the Univ. of Washington and Oregon State Univ., respectively. In particular, the author is grateful for the assistance of Jody Klymak in transferring the data and communicating associated technical details of the instruments.

P516524.PDF [Page: 12 of 44]

Table of contents

Abstract i

Résumé i

Executive summary iii

Sommaire iv

Acknowledgments v

Table of contents vi

List of Figures: vii

1. Introduction 1

2. Overview of the Physical Setting 2

3. Discussion of Echo-Sounder Data 6

4. Quantitative Zooplankton Scattering Levels 10

5. Prediction of Microstructure Scattering Levels 14

6. Conclusions and Recommendations 18

7. References: 21

Appendix 1: Crustacean Zooplankton Scattering Models 23

Appendix 2: Acoustic Scattering from Turbulent Microstructure 26

List of Figures:

Figure 1 Knight Inlet coastline in the vicinity of the sill at Hoeya Head. 2

Figure 2 Knight Inlet sill profile along track shown in upper plot, taken with 200 kHz echo-sounder on-board the *RV Miller*. 3

Figure 3 Tidal elevation vs. time (UTC) during the 1995 Knight Inlet experiment. Local standard time at this location is UTC – 8 hours. 3

Figure 4 Comparison of CTD profiles upstream (east) and downstream of the Knight Inlet sill during ebb tide, taken from the *CSS Vector* Aug. 24th, 1995. 4

Figure 5 Comparison of CTD profiles upstream (west) and downstream of the Knight Inlet sill during flood tide, taken from the CSS Vector Aug. 25th, 1995. 5

Figure 6 Temperature, salinity, and sigma-t from the Advanced Microstructure Profiler deployed from RV Miller, taken at 2257Z Sept 1st, 1995 at the eastern end of the Knight Inlet sill during flood tide. 5

Figure 7 Raw 200 kHz echo-sounder intensity vs. depth and time (seconds) starting 1715Z Aug. 23rd, 1995 from RV Miller heading from east to west across sill during daytime flood tide. Tidal flow is from right to left. White line indicates the detected seabed. 6

Figure 8 Raw 200 kHz echo-sounder intensity vs. depth and time (seconds) starting 1650Z Aug. 25th, 1995 from RV Miller heading from west to east across sill during daytime flood tide. Tidal flow is from left to right. White line indicates the detected seabed. 7

Figure 9 Raw 120 kHz echo-sounder intensity vs. depth and time (seconds) starting 0429Z Aug. 31st, 1995 from CSS Vector heading from east to west across sill during night-time ebb tide. Tidal flow is from left to right. White line indicates the detected seabed. 8

Figure 10 Raw 120 kHz echo-sounder intensity vs. depth and time (seconds) starting 0703Z Sept. 1st, 1995 from CSS Vector heading from east to west across sill at change from ebb to flood tide near midnight local time. Remnant ebb tidal flow is from left to right extending from sill crest near 50 to 60 m depth. White line indicates the detected seabed. 9

Figure 11 Comparison of backscattering spectra for typical Knight Inlet Euphausiids and Copepods. Vertical lines indicate echo-sounder frequencies used on the CSS Vector and RV Miller. 11

Figure 12 Averaged volume scatter strength profile at 200 kHz taken from the RV Miller at 1536Z, Aug. 23rd, 1995 roughly 1 km east of the sill. Raw data matched to zooplankton scattering strength using conversion of –153 dB. Noise floor given by $N(r) = -128.5 + 20\log[r]$. 12

P516524.PDF [Page: 14 of 44]

Figure 13 Time variation of acoustic backscatter profiles on western slope of the sill during flood tide, Aug. 25th, 1995. Volume scatter strength calculated using conversion factor found in Fig. 12. Profile plot colours correspond to time label colours on tidal height plot. Acoustic data averaged over 2 to 4 minute intervals where water depth was 125 to 140 m. 13

Figure 14 Raw 200 kHz echo-Sounder intensity vs. depth and time (seconds) starting 1514Z Aug. 30th, 1995 from RV Miller heading from east to west across sill during ebb tide. Tidal flow is from left to right. AMP profile 15770 indicated by white line near time = 600 s. 14

Figure 15 Advanced Microstructure Profiler data and comparison with 200 kHz echo-sounder at 1533Z Aug 30th, near eastern edge of sill during ebb tide. Seabed at 64 m. 16

Figure 16 Raw 200 kHz echo-Sounder intensity vs. depth and time (seconds) starting 2232Z Sept. 1st, from RV Miller heading from east to west across eastern side of sill during flood tide. Tidal flow is from right to left. AMP profiles indicated by lines at 600 and 1400 s. 16

Figure 17 Advanced Microstructure Profiler data and comparison with 200 kHz echo-sounder at 2257Z Sept 1st, near eastern edge of sill during flood tide. Seabed at 75 m. 17

Figure 18 Advanced Microstructure Profiler data and comparison with 200 kHz echo-sounder at 2245Z Sept 1st, on the eastern slope during flood tide. Seabed at 130 m. 17

1. Introduction

Knight Inlet, British Columbia is a remarkable natural laboratory for investigating the physics of stratified tidal flows and internal solitary waves. Additionally, it is expected that zooplankton populations in this area will exhibit significant behavioral responses to these complicated stratified flows. Several investigations of this area were conducted in the 1970's and '80's (e.g. Farmer and Smith 1980), and in August and September 1995 David Farmer of the Institute of Ocean Sciences (IOS) in Sidney, BC returned with a multi-disciplinary team to study the internal hydraulics of the tidal flows in this coastal fjord. The team included scientists from the Applied Physics Lab. at the Univ. of Washington (M. Gregg and E. d'Asaro) and from Scripps Institute of Oceanography (L. Armi). The IOS ship *CSS Vector* along with two smaller launches (the *RV Miller* and *RV Bazan Bay*) were used. A wide variety of oceanographic instrumentation was employed, including echo-sounders, acoustic Doppler current profilers, CTDs, and turbulent microstructure profilers. Although the primary focus of the 1995 experiments was the physical oceanography of stratified flows, as a by-product an impressive data set describing the distributions of zooplankton and fish was collected. This retrospective study summarizes what can be learned about the zooplankton behavior as a prelude to a more focused investigation in this same area in the fall of 2001.

High-frequency (HF, >30 kHz) echo-sounders are particularly useful for profiling abundance and behavior of zooplankton, which often occur with sufficiently high densities to be considered as quasi-continuous scattering layers or clouds rather than isolated targets. When used as an imaging tool, HF sounders can sample the water column beneath a vessel with high spatial-temporal resolution, of order a few cm in depth and 0.5 s between pings, to depths up to 400 m. When combined with new trawls and new GPS technology, quasi-synoptic surveys of zooplankton distributions are feasible. Furthermore, utilizing the zooplankton (and other particulates) as tracers, HF sounders provide a remarkable tool for flow visualization (e.g. Farmer and Armi 1999a,b).

Quantitatively, the acoustic backscatter strength as measured by a high-frequency echo-sounder is proportional to the zooplankton type and volumetric density. Unfortunately, the echo strength from a single frequency echo-sounder cannot distinguish in general between different zooplankton size classes (e.g. copepods and euphausiids). Furthermore, it has been found that single-frequency systems cannot distinguish in general between zooplankton and scattering from turbulent microstructure (Trevorrow 1998; Stanton et al. 1994a; Warren 2000). Given these facts, single-frequency systems are straight-forward to use only in non-turbulent environments dominated by a single species, or in situations where different zooplankton species can be distinguished on the basis of behavior. One solution to this problem is through the use of multiple frequencies, typically 50 to 2000 kHz, as demonstrated in many previous studies (e.g. Greenlaw 1977; Holliday & Pieper 1980; Trevorrow & Tanaka 1995; Warren 2000). Unfortunately, in this retrospective look we have data from only single frequency echo-sounders (120 and 200 kHz on two separate ships), and a co-occurrence of zooplankton with turbulent microstructure induced by the complicated flow over the sill. Furthermore, the HF sounders used in the 1995 experiments were not acoustically calibrated, and these 1995 field experiments lacked any direct sampling of the zooplankton population in Knight Inlet. In spite of these serious limitations, useful *qualitative* information on zooplankton distributions can be gleaned from the existing data, which should prove useful in designing zooplankton sampling strategies for the fall 2001 sea trials.

P516524.PDF [Page: 16 of 44]

2. Overview of the Physical Setting

Knight Inlet is a fjord located on the south-central coast of British Columbia, fed by a glacier at its head some 90 km inland, and open to the coastal Pacific through Queen Charlotte Sound at its mouth. Knight Inlet is relatively calm, with comparatively light winds and largely sheltered from oceanic wave action, making it ideal for field surveys. Overall, the lower part of Knight Inlet trends approximately WSW-ESE and has a roughly uniform width (see Figure 1). In this area the inlet is quite steep-sided, with side-wall slopes near 45° and mountain peaks on each side reaching over 1000 m above sea-level. In the middle of this lower section, between Hoeya Head and Prominent Point, there is an underwater sill running approximately North-South (i.e. roughly perpendicular to the East-West tidal flow) with typical depth near 60 m. Due to the geometry of the inlet in this sill region, near the center of the channel the flow regime has been found to be approximately 2-dimensional. This is shown by ADCP surveys in the sill region, and by aerial photographs of internal soliton crests forming straight lines as they propagate away from the sill (see Farmer and Armi 1999a).

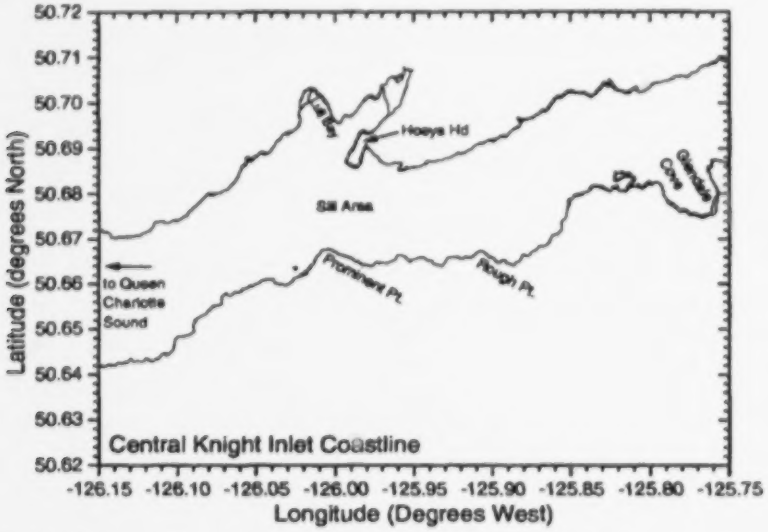

Figure 1 Knight Inlet coastline in the vicinity of the sill at Hoeya Head.

The bathymetric profile over the sill is asymmetric (see Figure 2), with the western side steeper than the eastern side and the sill top gradually sloping upwards towards the west. The bathymetric slope on the western side approaches 30%. To the west of the sill the seabed falls away to a flat bottom roughly 150 m deep, while on the eastern side there is a deeper basin with depths more than 400 m.

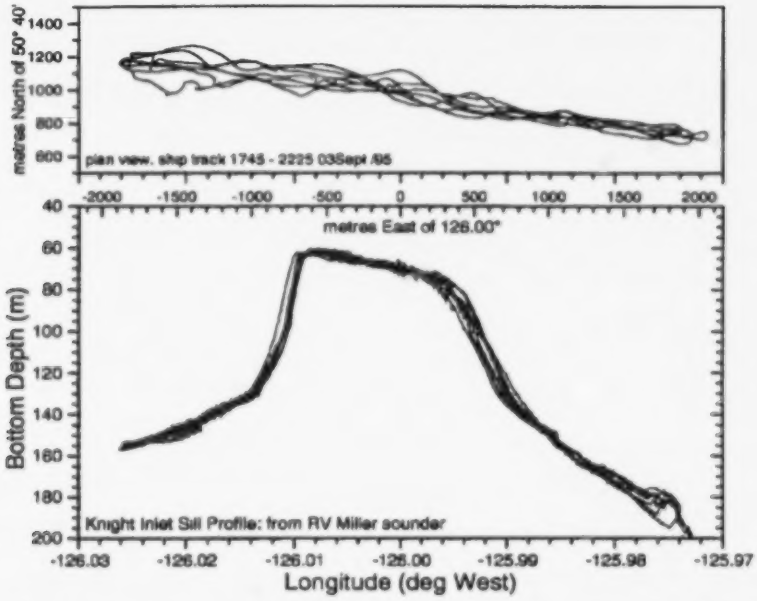
metres North of 50° 40'
plan view, ship track 1745 - 2225 03Sept.95
metres East of 126.00°
Bottom Depth (m)
Knight Inlet Sill Profile: from RV Miller sounder
Longitude (deg West)

Figure 2 Knight Inlet sill profile along track shown in upper plot, taken with 200 kHz echo-sounder on-board the *RV Miller*.

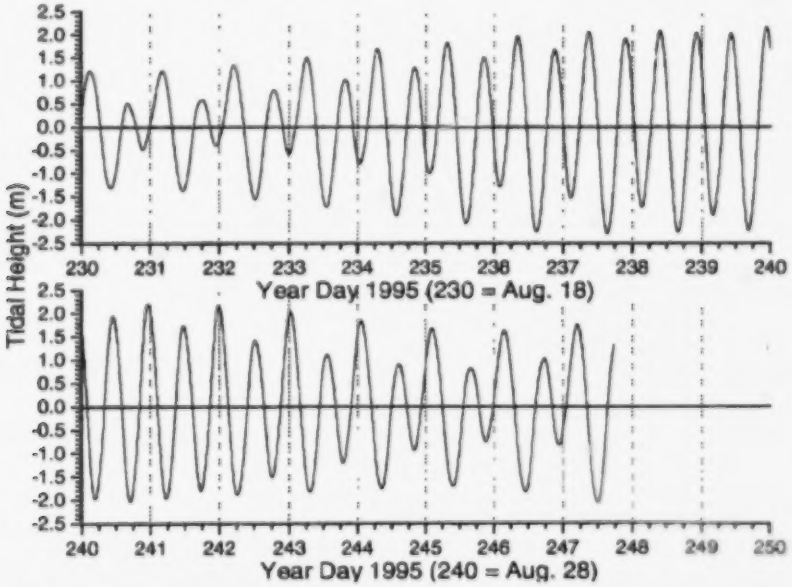

Figure 3 Tidal elevation vs. time (UTC) during the 1995 Knight Inlet experiment. Local standard time at this location is UTC – 8 hours.

P516524.PDF [Page: 18 of 44]

The area has dominantly semi-diurnal tides, with a strong fortnightly modulation and tidal heights ranging from 1.0 to 4.5 m. Figure 3 shows a tide gauge record taken near Rough Point (approximately 8 km east of the sill) during the 1995 experiments. Only negligible differences were found between this and a second tide gauge deployed approximately 2 km west of the sill, indicating that the sill has negligible effect on the tidal forcing. The flood tide runs eastward across the sill. Typical peak tidal currents over the sill (measured with ADCP from the CSS Vector) were near 1.2 $m \cdot s^{-1}$.

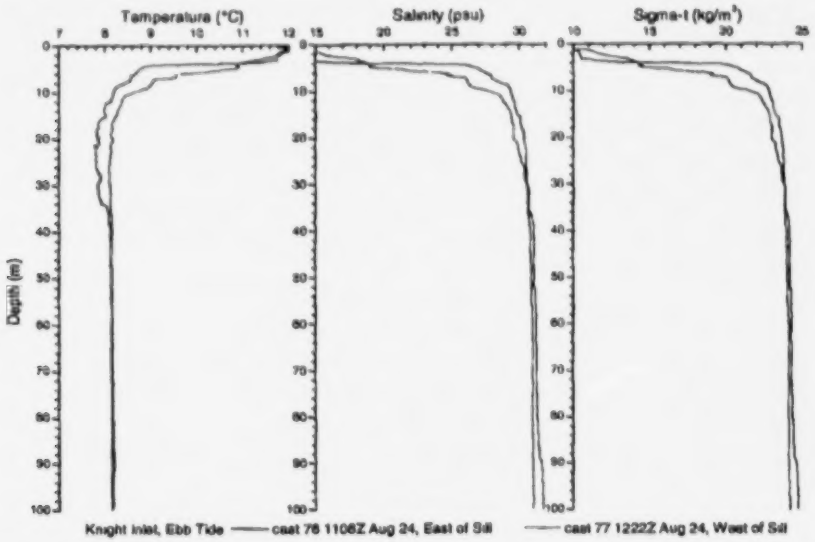
Temperature (°C)
Salinity (psu)
Sigma-t (kg/m³)
Depth (m)
Knight Inlet, Ebb Tide
cast 76 1106Z Aug 24, East of Sill
cast 77 1222Z Aug 24, West of Sill

Figure 4 Comparison of CTD profiles upstream (east) and downstream of the Knight Inlet sill during ebb tide, taken from the *CSS Vector* Aug. 24th, 1995.

During the late summer of 1995, Knight Inlet featured a strong near-surface stratification, with a warmer, fresher surface layer from 6 to 10 m deep with relatively well-mixed conditions in the deeper waters (see Figures 4 -6). Vertical gradients of temperature, salinity, and density across the interface were very strong (maxima approximately 2.0 $°C \cdot m^{-1}$, 8.6 $psu \cdot m^{-1}$, and 7.0 $kg \cdot m^{-4}$). Buoyancy frequency maxima near 0.15 to 0.3 $rad \cdot s^{-1}$ (85 to 170 $cycles \cdot hr^{-1}$) were found near 5 to 7 m depth. As shown in the upstream vs. downstream CTD comparisons (Figs. 4 and 5), the flow over the sill generated some mixing across these temperature-salinity gradients, on both ebb and flood tides. The depth of the pycnocline tended to be deeper on the downstream side. The deep waters (>50 m) in the eastern basin tend to be slightly fresher than on the west side of the sill. Over the top of the sill, distinct flow layers with very strong T-S gradients at the boundaries were commonly observed, often forming step-like structures (see Figure 6). These distinct flow boundaries were associated with strong velocity shear and turbulence.

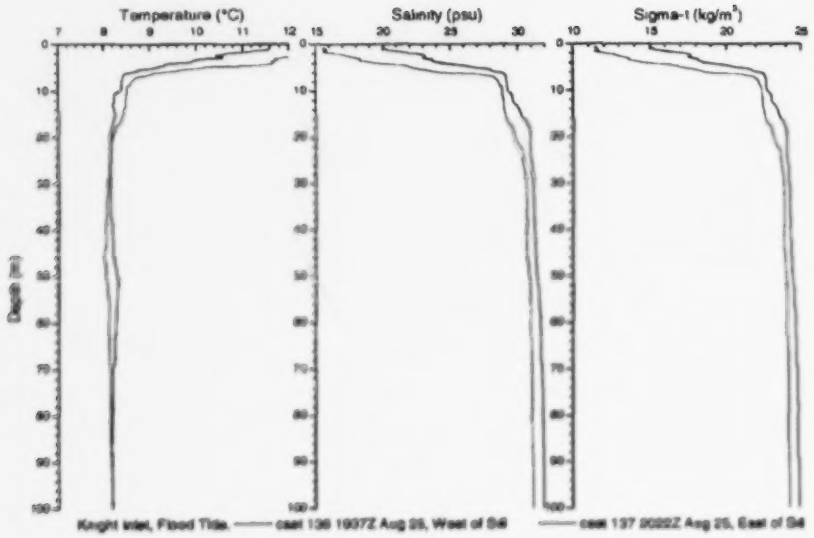

Figure 5 Comparison of CTD profiles upstream (west) and downstream of the Knight Inlet sill during flood tide, taken from the CSS Vector Aug. 25th, 1995.

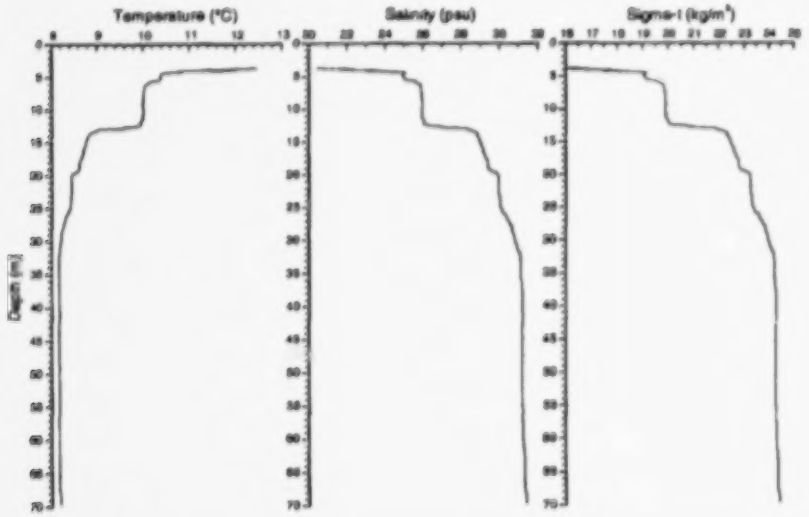

Figure 6 Temperature, salinity, and sigma-t from the Advanced Microstructure Profiler deployed from RV Miller, taken at 2257Z Sept 1st, 1995 at the eastern end of the Knight Inlet sill during flood tide.

3. Discussion of Echo-Sounder Data

The high-frequency echo-sounders used during the 1995 field surveys provided high spatial and temporal resolution imaging of the tidal flows and zooplankton distributions. Two BioSonics model 101 echo-sounders were used: a 200 kHz system mounted on the RV Miller, and a 120 kHz system deployed on a strut from the starboard side of the CSS Vector. Neither system was acoustically calibrated. The RV Miller system used a 4.5° beam-width transducer, transmitting a 0.5 ms pulse at a 1 Hz ping rate. Data was recorded within 12.5 cm bins to a typical depth of 200 m. The CSS Vector system used a 4.0° transducer, transmitting a 0.5 ms pulse at a 2 Hz ping rate, with sampling resolution of 6.8 cm to a depth of 150 m. Both systems digitized the raw echo with 16-bit resolution. For both sounders the 0.5 ms transmit pulse length defined an acoustic resolution of 37 cm. For display and further analysis the actual time-varying gains for both systems have been corrected to a $20\log[r] + \alpha r$ variation (where r = range and α = seawater absorption), thus the raw data is proportional to the volumetric scattering cross-section. RV Miller collected data during daylight hours only from Aug. 21st until Sept. 4th. The CSS Vector sounder was operated nearly continuously while the ship conducted surveys near the sill, and thus included both day and night-time data from Aug. 23rd until Sept. 5th. Typical vessel speeds during the surveys were 4 to 5 knots relative to the water. Figure 7-10, 14, and 16 show a few example echograms taken with these sounders.

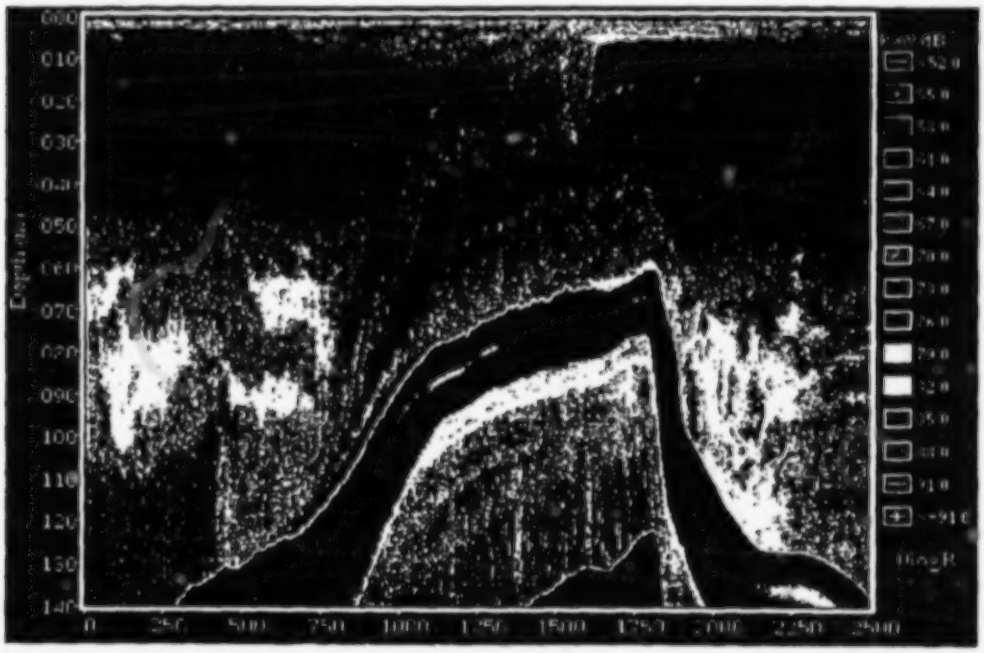

Figure 7 Raw 200 kHz echo-sounder intensity vs. depth and time (seconds) starting 1715Z Aug. 23rd, 1995 from RV Miller heading from east to west across sill during daytime flood tide. Tidal flow is from right to left. White line indicates the detected seabed.

During both flood and ebb tide there were strongly sheared internal hydraulic flows over the sill. A consistent feature of all acoustic echograms are strong and distinct *flow lines* within the upper 15 to 20 that correspond closely to strong vertical gradients of temperature and salinity. During flood tide (see Figures 7 and 8) a flow bifurcation commonly appeared over the sill, with a strong downward jet of water extending from about 15 m depth down the eastern slope to approximately 130 m. Downstream of the bifurcation there was a near-surface region of flow stagnation with active mixing along the boundaries. Along the interface of this downward flow, shear instabilities, undulations, and overturns were often observed (described by Farmer and Armi 1999a,b). For example in Fig. 7 the bifurcation point (near 1500s, 25m depth) was in the process of degenerating into an internal undular bore, which would be released westward when the tide turned. Also, Fig. 7 shows a small internal solitary wave train forming upstream of the bifurcation (near 2250s, 10m depth).

Figure 8 Raw 200 kHz echo-sounder intensity vs. depth and time (seconds) starting 1650Z Aug. 25th, 1995 from RV Miller heading from west to east across sill during daytime flood tide. Tidal flow is from left to right. White line indicates the detected seabed.

During the daytime, far away from the flow disturbances created by the sill, the zooplankton formed into dense layers between roughly 70 and 120 m depth, as shown in Figures 7 and 8. The daytime echograms generally showed very low background scattering levels between 20 and 60 m depth. There is some evidence from early mornings (around dawn) that this zooplankton layer was found shallower, near 30 to 50 m, with the depth quickly increasing suggestive of vertical migration. This behaviour and depth range suggests that the layer is dominantly composed of Euphausiids (krill), which are commonly found along the B.C. coast. Upstream of the sill the zooplankton layers appear to be trapped by the tidal flow against the steep western slope, forming a dense cloud near 100 m depth. On the downstream side of the

3. Discussion of Echo-Sounder Data

The high-frequency echo-sounders used during the 1995 field surveys provided high spatial and temporal resolution imaging of the tidal flows and zooplankton distributions. Two BioSonics model 101 echo-sounders were used: a 200 kHz system mounted on the RV Miller, and a 120 kHz system deployed on a strut from the starboard side of the CSS Vector. Neither system was acoustically calibrated. The RV Miller system used a 4.5° beam-width transducer, transmitting a 0.5 ms pulse at a 1 Hz ping rate. Data was recorded within 12.5 cm bins to a typical depth of 200 m. The CSS Vector system used a 4.0° transducer, transmitting a 0.5 ms pulse at a 2 Hz ping rate, with sampling resolution of 6.8 cm to a depth of 150 m. Both systems digitized the raw echo with 16-bit resolution. For both sounders the 0.5 ms transmit pulse length defined an acoustic resolution of 37 cm. For display and further analysis the actual time-varying gains for both systems have been corrected to a $20\log[r] + \alpha r$ variation (where r = range and α = seawater absorption), thus the raw data is proportional to the volumetric scattering cross-section. RV Miller collected data during daylight hours only from Aug. 21st until Sept. 4th. The CSS Vector sounder was operated nearly continuously while the ship conducted surveys near the sill, and thus included both day and night-time data from Aug. 23rd until Sept. 5th. Typical vessel speeds during the surveys were 4 to 5 knots relative to the water. Figure 7-10, 14, and 16 show a few example echograms taken with these sounders.

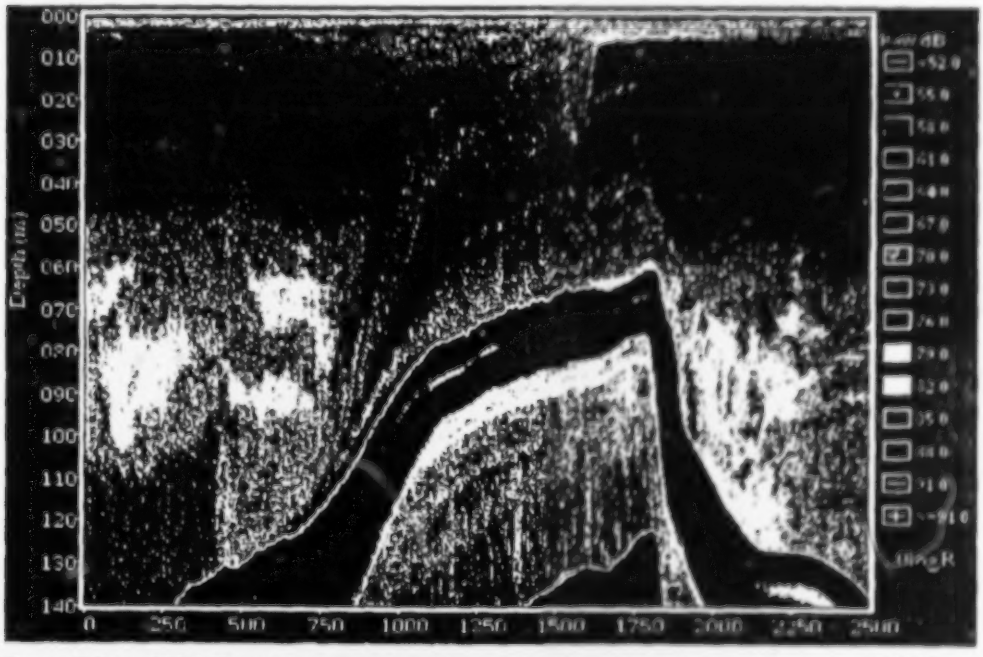

Figure 7 Raw 200 kHz echo-sounder intensity vs. depth and time (seconds) starting 1715Z Aug. 23rd, 1995 from RV Miller heading from east to west across sill during daytime flood tide. Tidal flow is from right to left. White line indicates the detected seabed.

During both flood and ebb tide there were strongly sheared internal hydraulic flows over the sill. A consistent feature of all acoustic echograms are strong and distinct *flow lines* within the upper 15 to 20 that correspond closely to strong vertical gradients of temperature and salinity. During flood tide (see Figures 7 and 8) a flow bifurcation commonly appeared over the sill, with a strong downward jet of water extending from about 15 m depth down the eastern slope to approximately 130 m. Downstream of the bifurcation there was a near-surface region of flow stagnation with active mixing along the boundaries. Along the interface of this downward flow, shear instabilities, undulations, and overturns were often observed (described by Farmer and Armi 1999a,b). For example in Fig. 7 the bifurcation point (near 1500s, 25m depth) was in the process of degenerating into an internal undular bore, which would be released westward when the tide turned. Also, Fig. 7 shows a small internal solitary wave train forming upstream of the bifurcation (near 2250s, 10m depth).

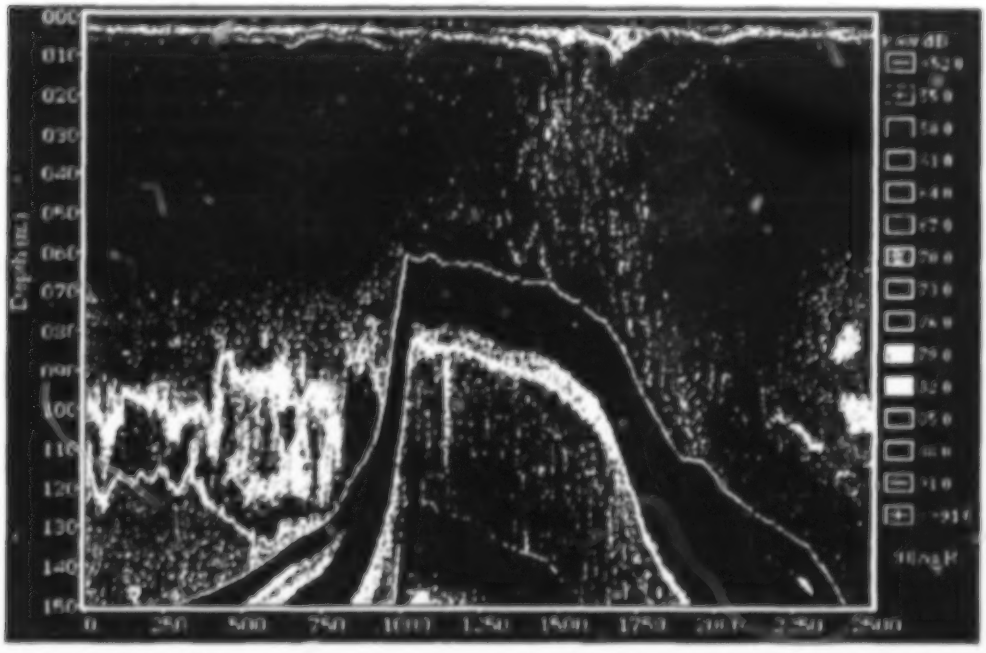

Figure 8 Raw 200 kHz echo-sounder intensity vs. depth and time (seconds) starting 1650Z Aug. 25th, 1995 from RV Miller heading from west to east across sill during daytime flood tide. Tidal flow is from left to right. White line indicates the detected seabed.

During the daytime, far away from the flow disturbances created by the sill, the zooplankton formed into dense layers between roughly 70 and 120 m depth, as shown in Figures 7 and 8. The daytime echograms generally showed very low background scattering levels between 20 and 60 m depth. There is some evidence from early mornings (around dawn) that this zooplankton layer was found shallower, near 30 to 50 m, with the depth quickly increasing suggestive of vertical migration. This behaviour and depth range suggests that the layer is dominantly composed of Euphausiids (krill), which are commonly found along the B.C. coast. Upstream of the sill the zooplankton layers appear to be trapped by the tidal flow against the steep western slope, forming a dense cloud near 100 m depth. On the downstream side of the

P516524.PDF [Page: 22 of 44]

sill, the zooplankton layer re-formed itself eastward and somewhat above the outlet of the down-welling jet. Both Figs. 7 and 8 reveal flow features that suggest zooplankton are being carried by the near-bottom currents up and over the sill crest. During day-time ebb tides (e.g. Figure 14) the overall zooplankton distributions were similar, however the upstream trapping was not quite so dramatic due to the shallower eastern slope.

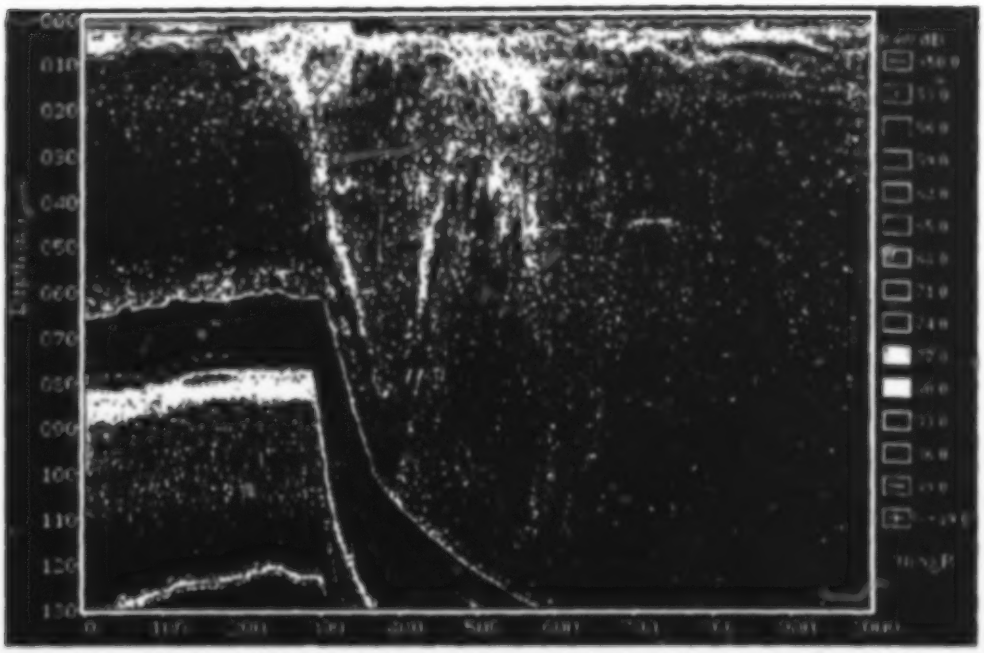

Figure 9 Raw 120 kHz echo-sounder intensity vs. depth and time (seconds) starting 0429Z Aug. 31st, 1995 from CSS Vector heading from east to west across sill during night-time ebb tide. Tidal flow is from left to right. White line indicates the detected seabed.

On the ebb tide a similar flow bifurcation always formed, usually centered over the western crest of the sill. Figs. 9 and 14 both show dramatic examples where the down-welling jet attached itself to the western slope down to depths of 100 to 120 m, then detached from the seabed and oscillated upwards. As in the flood tide case, shear instabilities (e.g. Fig. 9 near 200 s, 10 m depth) were commonly observed on the boundary of the down-welling jet, and internal solitary wave trains and/or internal bores were often released eastward as the tidal flow diminishes. Biologically, Figs. 9 and 10 show that at night-time the zooplankton and small fish were generally dispersed throughout the entire water column. Downstream of the sill the zooplankton did not condense into the 70 to 120 m layer as in the daytime, but rather remained dispersed. Figure 10 shows a dramatic example of zooplankton and fish dispersed throughout the entire water volume during night-time slack water (the fish appear as discrete streaks). In Fig. 10 the remnant ebb tidal flow appears as a horizontal jet centered at 60 m depth extending westward from the sill crest. However, there was some suggestion that even during night-time zooplankton also moved downwards to avoid being advected over the sill, for example shown by the near-bottom (55 to 60 m depth) zooplankton layers over the top of the sill in Fig. 9.

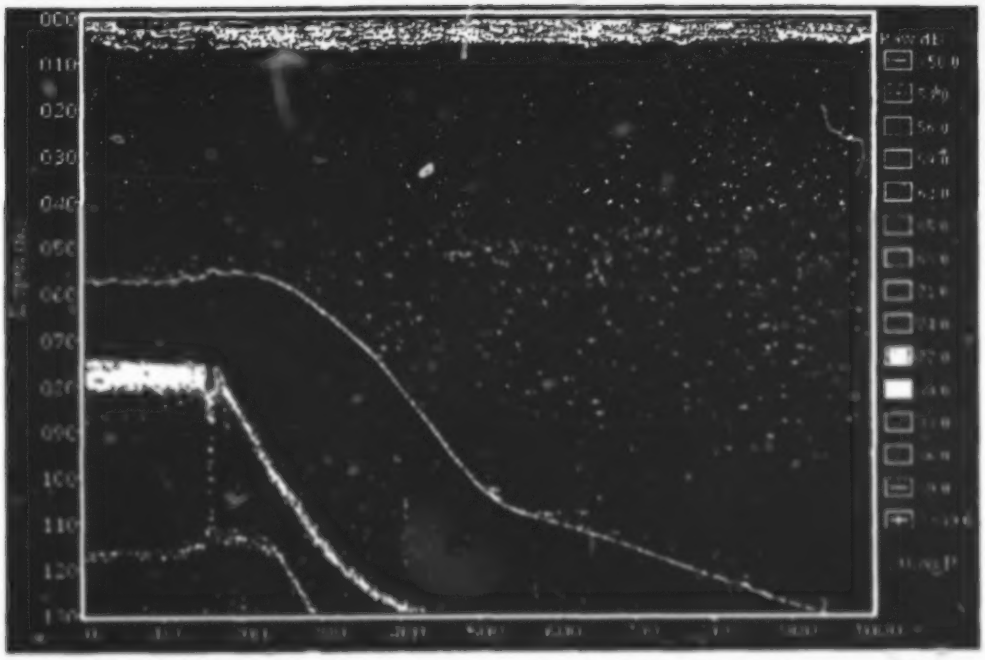

Figure 10 Raw 120 kHz echo-sounder intensity vs. depth and time (seconds) starting 0703Z Sept. 1st, 1995 from CSS Vector heading from east to west across sill at change from ebb to flood tide near midnight local time. Remnant ebb tidal flow is from left to right extending from sill crest near 50 to 60 m depth. White line indicates the detected seabed.

sill, the zooplankton layer re-formed itself eastward and somewhat above the outlet of the down-welling jet. Both Figs. 7 and 8 reveal flow features that suggest zooplankton are being carried by the near-bottom currents up and over the sill crest. During day-time ebb tides (e.g. Figure 14) the overall zooplankton distributions were similar, however the upstream trapping was not quite so dramatic due to the shallower eastern slope.

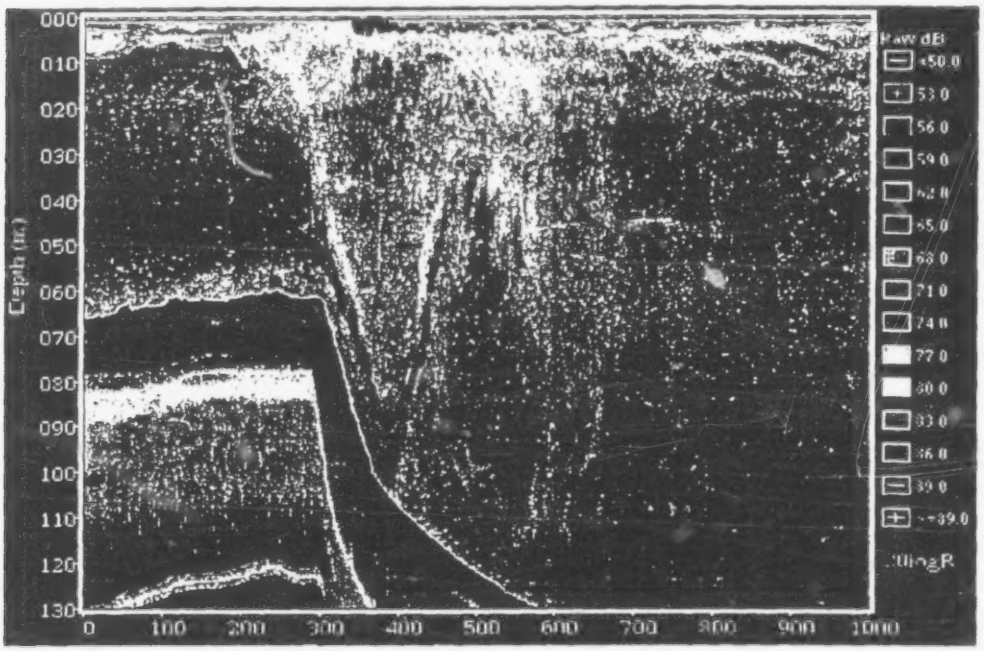

Figure 9 Raw 120 kHz echo-sounder intensity vs. depth and time (seconds) starting 0429Z Aug. 31st, 1995 from CSS Vector heading from east to west across sill during night-time ebb tide. Tidal flow is from left to right. White line indicates the detected seabed.

On the ebb tide a similar flow bifurcation always formed, usually centered over the western crest of the sill. Figs. 9 and 14 both show dramatic examples where the down-welling jet attached itself to the western slope down to depths of 100 to 120 m, then detached from the seabed and oscillated upwards. As in the flood tide case, shear instabilities (e.g. Fig. 9 near 200 s, 10 m depth) were commonly observed on the boundary of the down-welling jet, and internal solitary wave trains and/or internal bores were often released eastward as the tidal flow diminishes. Biologically, Figs. 9 and 10 show that at night-time the zooplankton and small fish were generally dispersed throughout the entire water column. Downstream of the sill the zooplankton did not condense into the 70 to 120 m layer as in the daytime, but rather remained dispersed. Figure 10 shows a dramatic example of zooplankton and fish dispersed throughout the entire water volume during night-time slack water (the fish appear as discrete streaks). In Fig. 10 the remnant ebb tidal flow appears as a horizontal jet centered at 60 m depth extending westward from the sill crest. However, there was some suggestion that even during night-time zooplankton also moved downwards to avoid being advected over the sill, for example shown by the near-bottom (55 to 60 m depth) zooplankton layers over the top of the sill in Fig. 9.

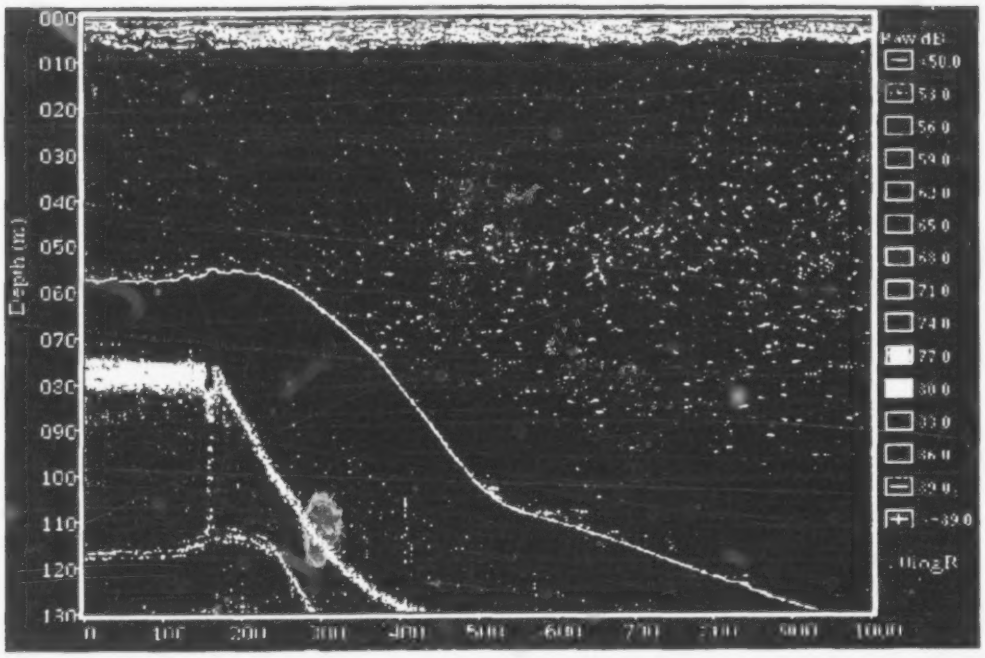

Figure 10 Raw 120 kHz echo-sounder intensity vs. depth and time (seconds) starting 0703Z Sept. 1st, 1995 from CSS Vector heading from east to west across sill at change from ebb to flood tide near midnight local time. Remnant ebb tidal flow is from left to right extending from sill crest near 50 to 60 m depth. White line indicates the detected seabed.

4. Quantitative Zooplankton Scattering Levels

It was expected that scattering layers observed with high-frequency echo-sounders in Knight Inlet, and particularly those exhibiting diurnal migrations, were composed of larger crustacean zooplankton such as euphausiids, copepods, amphipods, and various shrimp. Acoustic scattering models for these crustacean zooplankton are discussed in Appendix 1. Pieper (1971) found that deeper (80 to 120 m) daytime acoustic scattering layers in Saanich Inlet, BC were dominated by euphausiids (largely *Euphausia pacifica*), which are known to migrate to the surface at night. Also, Mackie & Mills (1983) reported dense (>100 per m^3) mid-water euphausiid layers from both net trawl and submersible observations in Saanich Inlet and other B.C. coastal areas. These studies reported typical adult *E. pacifica* lengths of 15 mm. The depth-extent of the euphausiids in Saanich Inlet was found to be limited by the 0.2 ml/litre oxycline near 80 to 100 m, however no such oxycline exists in Knight Inlet. The euphausiids are joined in their diurnal migrations by amphipods and larger shrimp, however these are generally found deeper or on the bottom during the day and migrate only to the mid-water during nighttime. Other species of Pteropods, Chaetognaths, Ctenophores, and Cnidaria (jellyfish) are known to migrate diurnally from the surface through depths of 250 m. However in the context of interpreting echo-sounding data these other species can be largely ignored due to their low abundance and small target strength (these are soft- or gelatinous-bodied animals). The exception to this are the hard shelled planktonic Pteropods *Limacina helicina* and *L. retroversa*, which for typical sized animals near 2 mm size have a *TS* at 200 kHz near –84 dB (Stanton et al. 1994b), more similar to that of small euphausiids. However, it is thought unlikely that significant numbers of these animals can be found in Knight Inlet. In summary, without detailed *in situ* samples it is impossible to know the relative abundances of these other species, and at this preliminary stage they will be ignored.

The most numerically abundant species in both the coastal and oceanic waters are Copepods, with adults reaching up to 3 to 4 mm in length. *Neocalanus plumchrus* appears to be the most common species in B.C. coastal waters. Dense aggregations of *N. plumchrus* has been observed at fronts in the nearby Strait of Georgia (Mackas & Louttit 1988). *Neocalanus spp.* generally do not migrate on a daily basis, but exhibit a pronounced seasonal growth and migration cycle. For example, young of *N. plumchrus* feeding on the spring bloom of phytoplankton grow rapidly in size and population in mid- and epi-pelagic zones (surface to 100 m) in the March through June period, then the adults dive to deep waters (>300 m) for the remainder of the year. Other smaller copepod species also exhibit seasonal migration cycles, generally peaking in abundance and size after the descent of *N. plumchrus* in June. Summer and fall near-surface blooms of *Calanus marshallae*, *C. pacificus*, *Pseudocalanus*, and *Metridia pacifica* are common in BC coastal waters (Harrison et al. 1983). Some of the other copepods (especially *M. pacifica*) do exhibit diurnal migration behaviour.

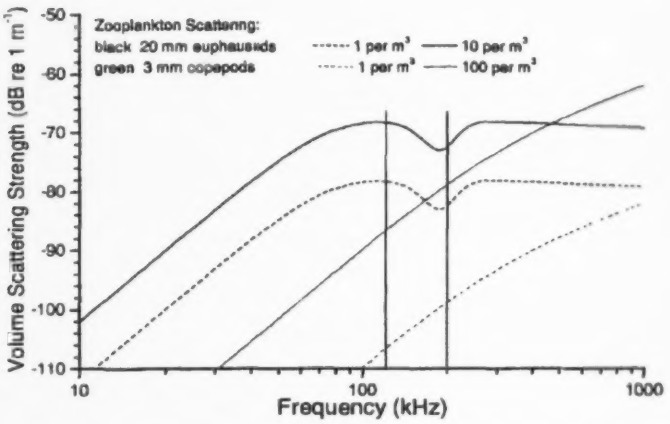

Figure 11 Comparison of backscattering spectra for typical Knight Inlet Euphausiids and Copepods. Vertical lines indicate echo-sounder frequencies used on the CSS Vector and RV Miller.

A comparison of the scattering strength vs. frequency for the two classes of zooplankton is shown in Figure 11 (the zooplankton scattering models are explained in Appendix 1). These models are based on fluid sphere and low-aspect ratio fluid cylinders, and thus have relatively low resolution. This is appropriate for averaging over natural distributions of zooplankter size and orientation. However, systematic variations in zooplankter orientation (e.g. animals diving in response to turbulence) have the potential to modify these predictions. This creates a need to measure in situ the zooplankter orientation. Fig. 11 shows that for typical animal densities, scattering from the larger euphausiids will dominate at frequencies below 300 kHz, whereas scattering from the more numerous copepods will dominate at higher frequencies. Since the echo-sounders used operated at 120 and 200kHz and the zooplankton layers exhibited diurnal migration behaviour, henceforth it shall be assumed that the observed zooplankton scattering was dominated by euphausiids.

An approximate calibration of the echo-sounders can be extracted by assuming a euphausiid density within layers that are clearly attributable to zooplankton. In particular, during daylight surveys the euphausiids were normally found in distinct layers between 60 and 100 m depth. Figure 12 shows a 60 s average echo-sounder intensity vs. depth profile converted to an approximate volume scatter strength. The euphausiid layer is clearly visible. Assuming euphausiid densities of 10 to 20 per m^3 produces a rough conversion factor of –155 dB, which is a reasonable value for this instrument. Also, this conversion factor produces results consistent with a microstructure scattering model, as described in the next section. Clearly, this rough conversion factor *cannot* be used to make quantitative estimates of zooplankton densities – this requires a proper calibration. It is conceivable that echo-statistical methods, similar to those described in Trevorrow & Tanaka (1997), could be used to extract a calibration conversion factor. However, this statistical approach would require that *in situ* samples of the euphausiids had been taken during these 1995 field surveys, which was unfortunately not done. Also apparent in these data are regions where the echo is dominated by background noise, both acoustic and electrical, that is increased by the echo-sounder time-varying gain. An estimate of the noise vs. range curve was generated by fitting a curve of the

form 20log[r] + *constant* to the noise regions of the backscatter profile up to 400 m range, including echoes from below the main seabed echo. Clearly, in Fig. 12 the echo from 110 m to the seabed (at 180 m) is noise-dominated.

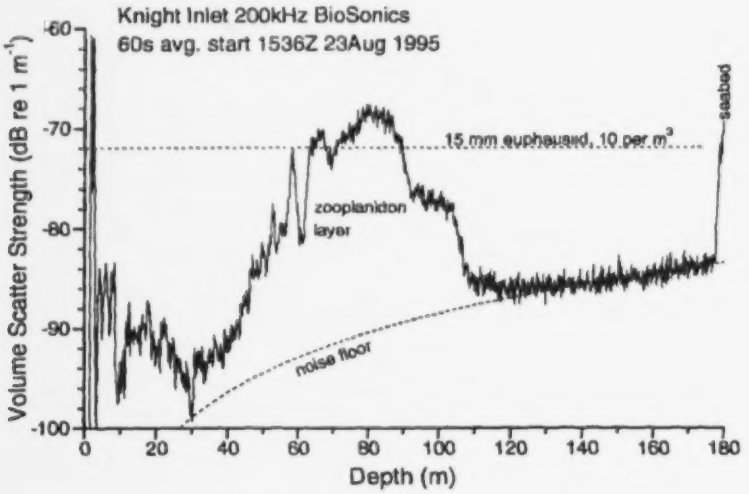

Figure 12 Averaged volume scatter strength profile at 200 kHz taken from the RV Miller at 1536Z, Aug. 23rd, 1995 roughly 1 km east of the sill. Raw data matched to zooplankton scattering strength using conversion of –153 dB. Noise floor given by N(r) = -128.5 + 20log[r].

Regardless of the calibration uncertainty, these volume scattering profiles can be used to show relative changes in zooplankton abundance. An example of this is shown in Figure 13 by the temporal variation during flood tide on the western slope of the sill. On this day the RV Miller made frequent crossings of the sill along the same track, and by extracting profiles at the same location (in this case extracted where the water depth was 125 to 140 m) time sequences can be created. Fig. 13 shows the build up of a zooplankton cloud from 90 to 120 m trapped on the western slope of the sill by the current. A 10 to 15 dB increase in zooplankton density at depths of 100 - 120 m occurs between low-water slack and mid-tide (near 2000h), while at the same time in the mid-waters (20 to 80m) the density actually decreases. This mid-water decrease could be due to some combination of the zooplankton moving downwards and advection of zooplankton-free waters from further upstream. As the tidal current eases towards high-water slack (2200h), the near-bottom zooplankton density drops by 15 to 25 dB (note change between 2000h and 2059h near 110 m depth), in some regions approaching the noise threshold. Closer examination of the echograms just before high-water slack suggests that the zooplankton clouds have moved westwards away from the sill.

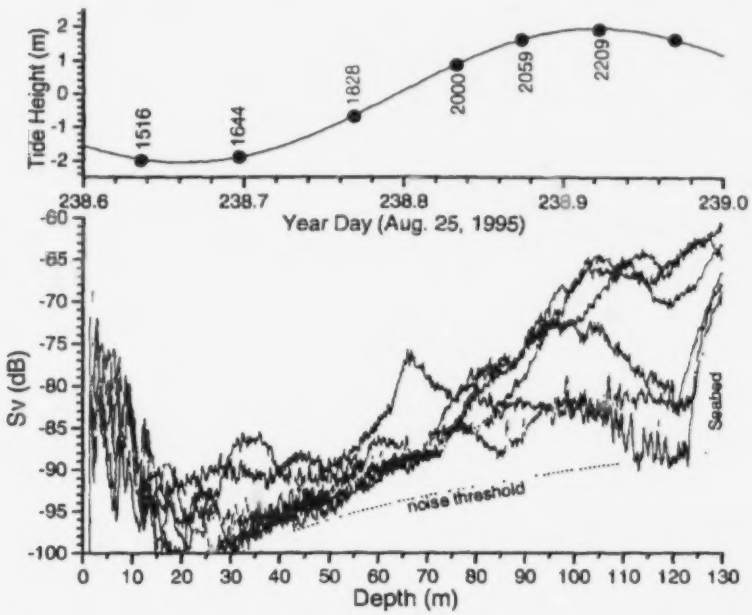

Figure 13 Time variation of acoustic backscatter profiles on western slope of the sill during flood tide, Aug. 25th, 1995. Volume scatter strength calculated using conversion factor found in Fig. 12. Profile plot colours correspond to time label colours on tidal height plot. Acoustic data averaged over 2 to 4 minute intervals where water depth was 125 to 140 m.

5. Prediction of Microstructure Scattering Levels

Another possible source of acoustic backscattering is turbulent microstructure created within regions of strong current shear found in the internal hydraulic flows over the sill. Measurements of similar microstructure scattering within internal solitons have been reported previously by Sandstrom et al. (1989) and Trevorrow (1998). In this present study some direct microstructure measurements were made using the Advanced Microstructure Profiler (AMP, for technical details see Wesson and Gregg 1994) deployed from the RV Miller. Thus comparisons between the observed acoustic scattering and predicted microstructure scattering levels can be made. An outline of the acoustic scattering model for turbulent microstructure is given in Appendix 2. This model requires as input the turbulence dissipation rate, ε, the buoyancy frequency, N, and gradients of temperature and salinity.

Figure 14 Raw 200 kHz echo-Sounder intensity vs. depth and time (seconds) starting 1514Z Aug. 30th, 1995 from RV Miller heading from east to west across sill during ebb tide. Tidal flow is from left to right. AMP profile 15770 indicated by white line near time = 600 s.

The AMP instrument was deployed in a free-fall mode from the RV Miller while simultaneously conducting echo-sounder surveys. AMP measures high-resolution temperature, salinity, and velocity shear as a function of depth. Estimates of ε, N, dT/dz, and dS/dz were then extracted within 0.5 m depth bins. AMP falls vertically with a terminal speed near 70 $cm \cdot s^{-1}$, and thus required roughly 50 to 200 s per cast, during which time the profiler was horizontally advected by the currents. Thus, comparisons of AMP profiles require extraction of the acoustic data along the profiler trajectory, using knowledge of the vessel and

5. Prediction of Microstructure Scattering Levels

Another possible source of acoustic backscattering is turbulent microstructure created within regions of strong current shear found in the internal hydraulic flows over the sill. Measurements of similar microstructure scattering within internal solitons have been reported previously by Sandstrom et al. (1989) and Trevorrow (1998). In this present study some direct microstructure measurements were made using the Advanced Microstructure Profiler (AMP, for technical details see Wesson and Gregg 1994) deployed from the RV Miller. Thus comparisons between the observed acoustic scattering and predicted microstructure scattering levels can be made. An outline of the acoustic scattering model for turbulent microstructure is given in Appendix 2. This model requires as input the turbulence dissipation rate, ε, the buoyancy frequency, N, and gradients of temperature and salinity.

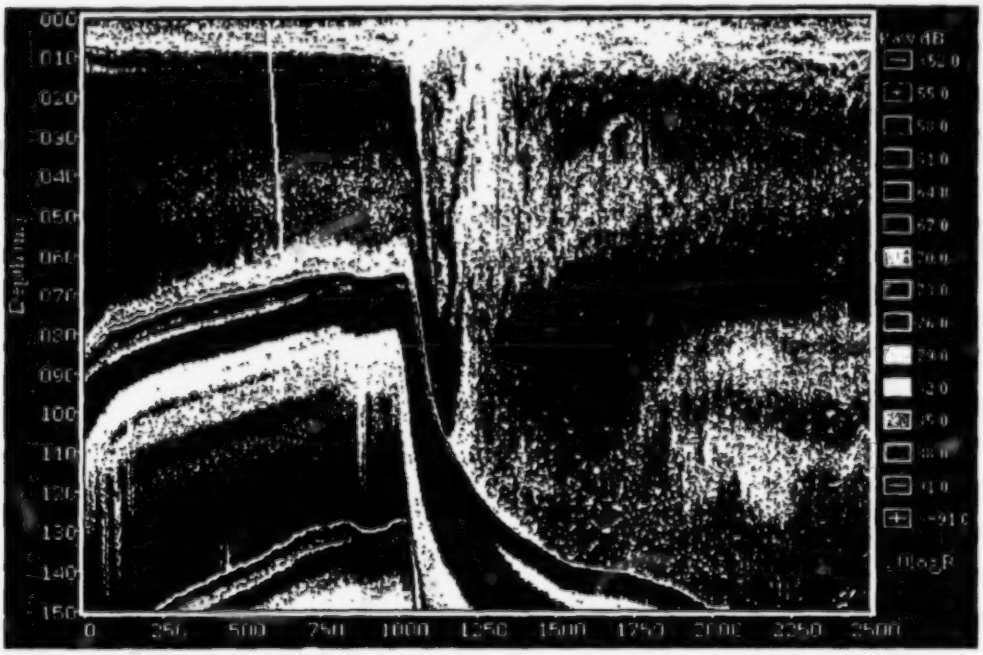

Figure 14 Raw 200 kHz echo-Sounder intensity vs. depth and time (seconds) starting 1514Z Aug. 30th, 1995 from RV Miller heading from east to west across sill during ebb tide. Tidal flow is from left to right. AMP profile 15770 indicated by white line near time = 600 s.

The AMP instrument was deployed in a free-fall mode from the RV Miller while simultaneously conducting echo-sounder surveys. AMP measures high-resolution temperature, salinity, and velocity shear as a function of depth. Estimates of ε, N, dT/dz, and dS/dz were then extracted within 0.5 m depth bins. AMP falls vertically with a terminal speed near 70 $cm \cdot s^{-1}$, and thus required roughly 50 to 200 s per cast, during which time the profiler was horizontally advected by the currents. Thus, comparisons of AMP profiles require extraction of the acoustic data along the profiler trajectory, using knowledge of the vessel and

water velocities. In this preliminary analysis a uniform water velocity profile was assumed, with the vessel speed taken from GPS.

Figures 14 and 15 show the echo-sounder and AMP profile data for a cast taken near the sill crest during ebb tide on Aug. 30th. The echo-sounder image shows the usual internal flow bifurcation above the sill crest, with a strong down-welling jet on the western side of the sill. The AMP profile crossed several distinct linear features within the upper 20 m before plunging through more diffuse scattering regions likely composed of zooplankton. In particular, the relatively dense layer near the seabed on the top of the sill has similar level and texture to the cloudlike zooplankton structure downstream of the sill at depths of 80 to 130 m. Through comparison with the AMP data (Fig. 15), it can be seen that these distinct *flow lines* observed with the echo-sounder correspond to strong temperature and salinity gradients (near -0.8 °C·m^{-1}and 2.3 psu·m^{-1}), and to maximal values of ε, χ, and N. Within the two strongest layers near 4 and 10 m depth there is good agreement between the acoustic data and the predicted microstructure scattering intensity (using the approximate acoustic conversion factor discussed previously). Note that within these near-surface layers the ratio of temperature to salinity gradients (δ) is quite stable at a value near -0.2. This indicates that temperature and salinity contributions to the microstructure scattering are of roughly equal importance, keeping in mind that the temperature effects on sound speed are approximately 3 times greater than salinity effects. At depths >15 m the gradients of temperature and salinity became quite small (magnitude $<10^{-3}$ in both cases), leading to instabilities in the ratio of these gradients as they oscillated around zero. However at these greater depths the measured ε, and thus the predicted microstructure scattering, was negligible. This further reinforces the conclusion that the deeper volume scattering is due to zooplankton. The AMP profile stopped short of the bottom boundary layer (to prevent damage), so that definite conclusions about the source of the strong acoustic scattering observed near 60 m depth on the top of the sill cannot be drawn.

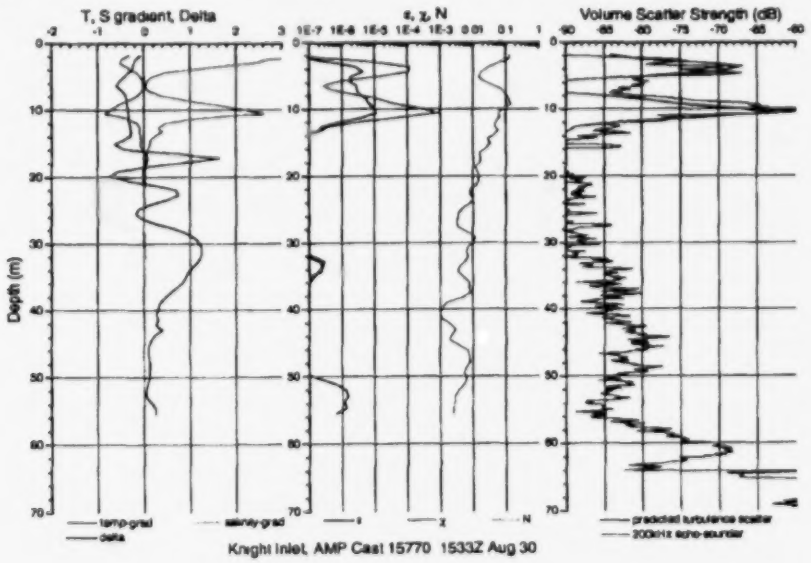

Figure 15 Advanced Microstructure Profiler data and comparison with 200 kHz echo-sounder at 1533Z Aug 30th, near eastern edge of sill during ebb tide. Seabed at 64 m.

Figures 16 - 18 show two more example echo-sounder vs. AMP comparisons taken near the eastern end of the sill during flood tide. In this situation the flow did not show a strong bifurcation, but rather a gradual deepening and expansion of the flow lines as they spilled down the eastern slope. Similar to the previous example, the strong flow lines near the surface in the echo-sounder data correspond to strong temperature and salinity gradients and maximal values of ε, χ, and N. In Fig. 17 the predicted microstructure scattering within layers at 5, 12, and 19 m depth is in moderate agreement with the acoustic scattering data. The downstream profile (Fig. 18) shows good agreement for the layer at 9 m depth, and furthermore the microstructure scattering prediction suggests that acoustic scattering in the 20 to 45 m depth region could also be attributable to turbulence. Similar to the earlier example, below the surface stratification the predicted microstructure scattering is negligible, due to either small dissipation rates or small temperature and salinity gradients, or both. This leads to the assertion that in these deeper regions the observed acoustic scattering levels must be due to zooplankton. At the top of the sill the AMP profile stopped short of the bottom boundary layer, so the source of the acoustic scattering layer near 70 m depth cannot be unambiguously identified. In the downstream profile the AMP data extended to very near the bottom, showing very little sign of microstructure scattering contributions. However in this case the near-bottom acoustic scattering layer also diminished

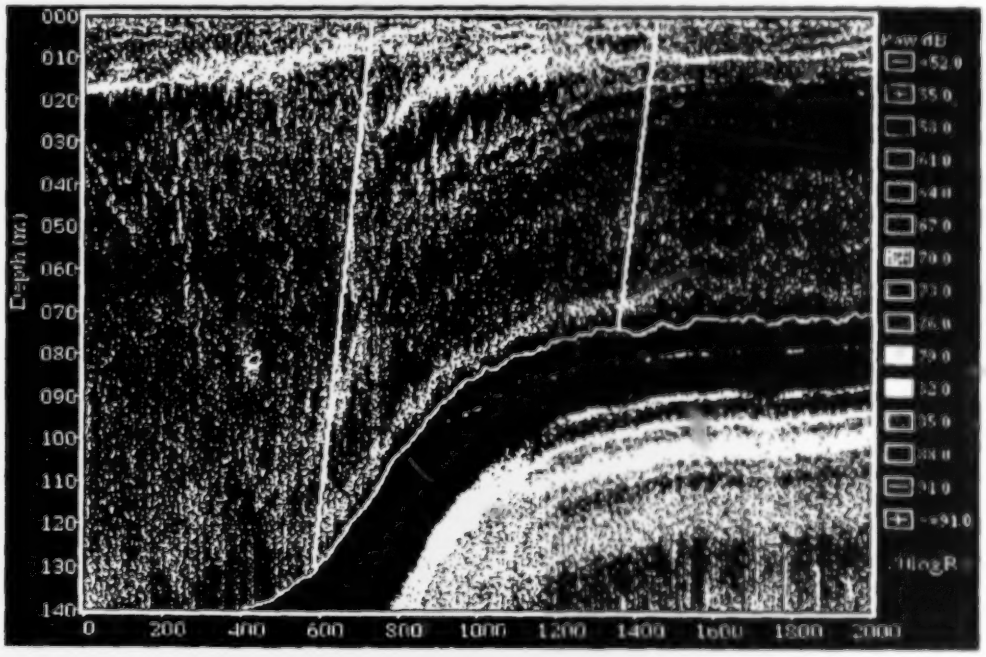

Figure 16 Raw 200 kHz echo-Sounder intensity vs. depth and time (seconds) starting 2232Z Sept. 1st, from RV Miller heading from east to west across eastern side of sill during flood tide. Tidal flow is from right to left. AMP profiles indicated by lines at 600 and 1400 s.

P516524.PDF [Page: 30 of 44]

Figure 15 Advanced Microstructure Profiler data and comparison with 200 kHz echo-sounder at 1533Z Aug 30th, near eastern edge of sill during ebb tide. Seabed at 64 m.

Figures 16 - 18 show two more example echo-sounder vs. AMP comparisons taken near the eastern end of the sill during flood tide. In this situation the flow did not show a strong bifurcation, but rather a gradual deepening and expansion of the flow lines as they spilled down the eastern slope. Similar to the previous example, the strong flow lines near the surface in the echo-sounder data correspond to strong temperature and salinity gradients and maximal values of ε, χ, and N. In Fig. 17 the predicted microstructure scattering within layers at 5, 12, and 19 m depth is in moderate agreement with the acoustic scattering data. The downstream profile (Fig. 18) shows good agreement for the layer at 9 m depth, and furthermore the microstructure scattering prediction suggests that acoustic scattering in the 20 to 45 m depth region could also be attributable to turbulence. Similar to the earlier example, below the surface stratification the predicted microstructure scattering is negligible, due to either small dissipation rates or small temperature and salinity gradients, or both. This leads to the assertion that in these deeper regions the observed acoustic scattering levels must be due to zooplankton. At the top of the sill the AMP profile stopped short of the bottom boundary layer, so the source of the acoustic scattering layer near 70 m depth cannot be unambiguously identified. In the downstream profile the AMP data extended to very near the bottom, showing very little sign of microstructure scattering contributions. However in this case the near-bottom acoustic scattering layer also diminished

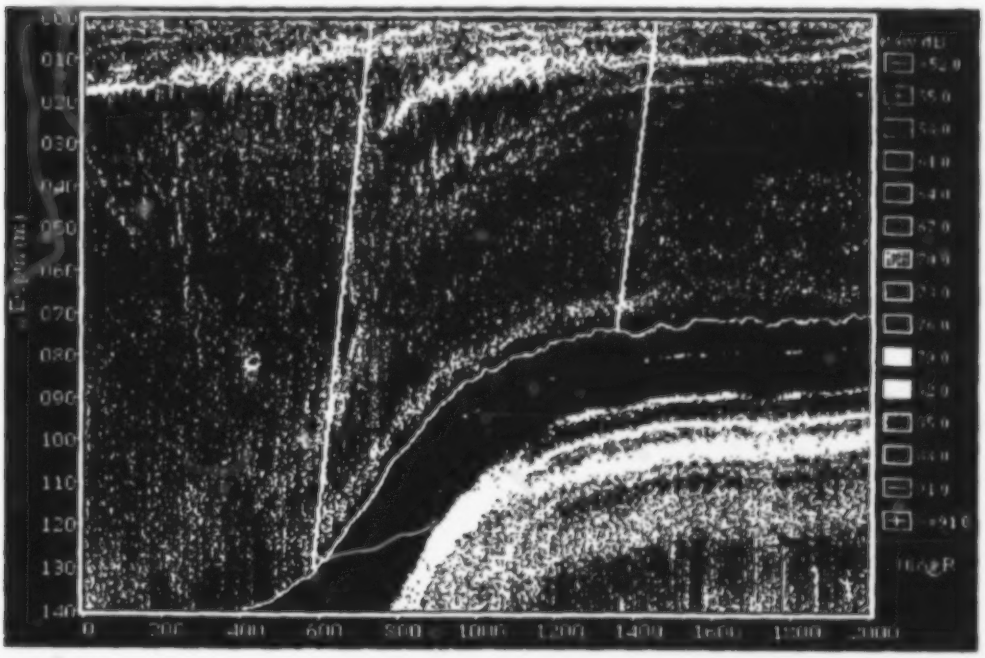

Figure 16 Raw 200 kHz echo-Sounder intensity vs. depth and time (seconds) starting 2232Z Sept. 1st, from RV Miller heading from east to west across eastern side of sill during flood tide. Tidal flow is from right to left. AMP profiles indicated by lines at 600 and 1400 s.

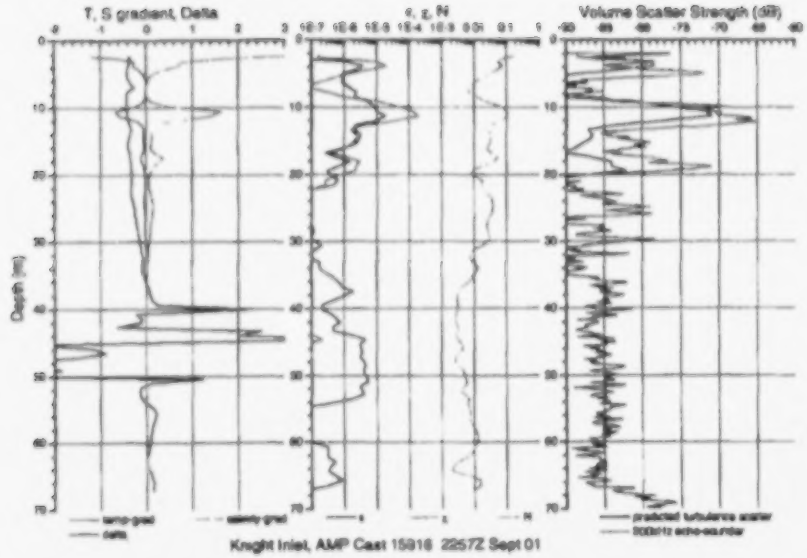

Figure 17 Advanced Microstructure Profiler data and comparison with 200 kHz echo-sounder at 2257Z Sept 1st, near eastern edge of sill during flood tide. Seabed at 75 m.

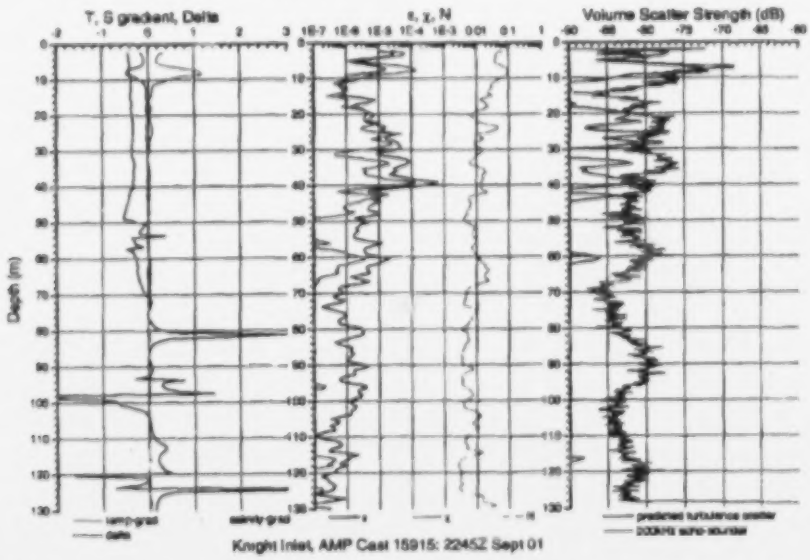

Figure 18 Advanced Microstructure Profiler data and comparison with 200 kHz echo-sounder at 2245Z Sept 1st, on the eastern slope during flood tide. Seabed at 130 m.

6. Conclusions and Recommendations

The high-resolution vessel-based echo-sounders used in the 1995 surveys produced dramatic images of complex internal hydraulic flows, turbulence, and zooplankton distributions in the vicinity of the Knight Inlet sill. The addition of high-resolution *in situ* current (ADCP) and water property (CTD and turbulence) profiles allowed some interpretation of the echo-sounder image features, including assessment of the flow internal hydraulics (see e.g. Farmer and Armi 1999a,b) and identification of acoustic scattering regions attributable to either zooplankton and turbulent microstructure. This retrospective look has found that the general zooplankton distributions were modified only modestly by the turbulent internal hydraulic flows over the sill. The zooplankton retained their classic diurnal migration habits, forming into relatively dense layers at 70 to 120 m depth during the day and dispersing throughout the entire water column at night. This behaviour is suggestive that these zooplankton are dominantly Euphausiids, which are common in B.C. coastal inlets such as Knight Inlet. During the day on both ebb and flood tides, there was evidence that the zooplankton layers were trapped and concentrated by the flow against the upstream side of the sill (which projects above this daytime scattering layer). It is thought that some zooplankton were caught by the flow and advected up and over the sill, re-forming the usual scattering layer again downstream of the sill. At night, and particularly during periods of slack water, the zooplankton and small fish were seen dispersed throughout the water column with seemingly little regard for the internal tidal flows. There was some suggestion that during night-time upstream of the sill some zooplankters attempted to dive to the seabed to avoid being caught in the intensely turbulent flows, ending up as bottom-hugging layers near the sill crest.

A comparison of acoustic scattering with the *in situ* temperature, salinity, and turbulence profiles suggests that microstructure scattering was responsible for the *flow lines* appearing in the strongly stratified near-surface region (upper 20 m). In particular, over the crest of the sill the flow often separated into distinct layers with strong pycnoclines and current shear at the boundaries. The acoustically-imaged flow lines corresponded directly to these pycnoclines and turbulence maxima. Through the use of microstructure scattering models scattering levels were predicted along these boundaries which were roughly consistent with the acoustic measurements. Outside of the these strongly stratified layers, the predicted microstructure scattering was small or negligible due to either small temperature and salinity gradients or small turbulence dissipation rates, or both. This left only zooplankton (in general) as the source of acoustic scattering throughout the bulk of the deeper waters.

A great deal more could have been done with the acoustic data reported herein if either of the two echo-sounders had been acoustically calibrated. Such calibrations would have allowed quantitative assessment of zooplankton abundances and some verification of the microstructure scattering models. Alternately, an acoustic calibration (raw intensity to biomass) could have been extracted if co-located net trawls to determine zooplankton abundance had been collected. Even if only a few samples of the zooplankton had been collected for the purposes of species identification and length-biomass measures, an acoustic calibration could have been extracted using critical density analysis of the echo-amplitude statistics (see Trevorrow & Tanaka 1997). As none of this was done (the 1995 study was focused on internal flow hydrodynamics, not bio-acoustics), the only avenue remaining was to estimate a rough ($\pm$ 5 to 10 dB) calibration assuming a euphausiid size of 15 mm and density of 10 to 20 per m^3 within daytime deep scattering layers. This rough calibration factor

produced estimates of acoustic microstructure scattering that were consistent with models based on *in situ* T, S, and turbulence dissipation measurements. However, this cannot be construed as a verification of the scattering model, but rather a suggestion that the analysis is on the right track.

Summarizing the acoustic scattering models presented in Sections 4 and 5, at frequencies in the 50 to 500 kHz range the predicted microstructure scattering spectra have a similar level and shape to the predicted zooplankton (i.e. euphausiid and copepod) spectra. This makes it difficult to distinguish between the two mechanisms solely on the basis of scattering strength. Acquiring high-resolution temperature, salinity, and microstructure measurements simultaneous and co-located with the acoustic sounding is necessary to identify regions where turbulence is present. On the acoustic side, a multi-frequency approach would seem to be the obvious solution. At a minimum two echo-sounder frequencies should be used, one operating in the 10 - 50 kHz range and the other at 100 - 200 kHz. At or below 50 kHz the zooplankton scattering should be greatly reduced relative to the microstructure scattering level.

In addition to the above mentioned requirements for acoustic calibration, direct turbulence measurements, and *in situ* zooplankton sampling, this study suggests a number of hypotheses which should be investigated in future field surveys, namely:

1. It was asserted that the zooplankton clouds observed during daylight at 70 to 120 m depth were dominated by Euphausiids (largely *E. pacifica*), with other species making negligible contributions to the acoustic scattering. It was further assumed that zooplankton abundances were low or negligible within the strongly stratified upper layers during the day. Net trawls and in situ sampling are clearly necessary.
2. Simple fluid sphere and cylinder models for the zooplankton scattering were proposed, based on previous modeling and measurement work. It was asserted that these models were appropriate for measuring average scattering levels over populations with some variation in size and orientation. Clearly, it is necessary to investigate the validity of these models, through both net trawls to establish abundances and animal sizes, and through some form of *in situ* monitoring of animal orientation. Acoustic measurements at several frequencies are required.
3. During daylight, it was speculated that some zooplankton from the pool trapped against the upstream slope were caught by the currents and carried up and over the sill, creating the observed near-bottom layer flowing over the sill crest. Both diel and nocturnal advection over the sill would homogenize the zooplankton populations on opposite sides of the sill. A competing hypothesis is that this near-bottom layer is a result of bottom boundary-layer turbulence, and that zooplankton are not advected over the sill during daytime. Simultaneous net and acoustic surveys overtop of the sill would shed light on this.
4. It was tentatively concluded that the distinct flow lines observed with the echo-sounder were due to turbulent microstructure scattering, with negligible contributions from zooplankton within these regions. Conversely, predicted microstructure scattering levels were negligible outside of these highly stratified zones, leading to the conclusion that zooplankton scattering dominated over the bulk of the water column. However, these conclusions are based on microstructure scattering models that have never been adequately field tested. Future efforts should be placed in establishing some confidence in these models, particularly measuring the frequency dependence of the turbulence

scattering. Ultimately this may provide the means to discriminate acoustically between turbulence and zooplankton scattering.

5. Very high levels of acoustic scattering were observed within the near-surface region (depths <10m), above the main pycnocline and away from zones of high turbulence. This scattering is possibly of biological origin, but the exact source is unknown. Near-surface zooplankton samples are necessary.

7. References:

Farmer, D., and J. D. Smith, 1980. Tidal interaction of stratified flow with a sill in Knight Inlet, *Deep-Sea Res.* **27A**: 329-254.

Farmer, D., and L. Armi, 1999a. The generation and trapping of solitary waves over topography, *Science* **283**: 188-190.

Farmer, D., and L. Armi, 1999b. Stratified flow over topography: the role of small-scale entrainment and mixing in flow establishment. *Proc. Roy. Soc. Lond.* **A455**: 3221-3258.

Greene, C., P. Wiebe, and J. Burczynski, 1989. Analyzing zooplankton size distributions using high-frequency sound, *Limnol. Oceanogr.* **34**(1): 129-139.

Greenlaw, C., 1977. Backscattering spectra of preserved zooplankton, *J. Acoust. Soc. Am.* **62**(1): 44-52.

Harrison, P., J. Fulton, F. Taylor, and T. Parsons, 1983. Review of the biological oceanography of the Strait of Georgia: pelagic environment, *Can. J. Fish. Aquat. Sci.* **40**: 1064-1094.

Holliday, D. V., and R. Pieper, 1980. Volume scattering strengths and zooplankton distributions at acoustic frequencies between 0.5 and 3 MHz, *J. Acoust. Soc. Am.* **67**(1): 135-146.

Johnson, R., 1977. Sound scattering from a fluid sphere revisited, *J. Acoust. Soc. Am.*, **61**: 375-377.

Kristensen, A., and J. Dahlen, 1986. Acoustic estimation of size distributions and abundance of zooplankton, *J. Acoust. Soc. Am.* **80**(2): 601-611.

Mackas, D., and G. Louttit, 1988. Aggregation of the copepod *Neocalanus plumchrus* at the margin of the Fraser River in the Strait of Georgia, *Bull. Mar. Sci.* **43**(3): 810-824.

Mackie, G., and C. Mills, 1983. Use of the Pisces IV submersible for zooplankton studies in coastal waters of British Columbia. *Can. J. Fish. Aquat. Sci.* **40**: 763-776.

Pieper, R., 1971. A study of the relationship between zooplankton and high-frequency scattering of underwater sound, Ph.D. dissertation, Univ. of British Columbia.

Seim, H., M. Gregg, and R. Miyamoto, 1995. Acoustic backscatter from turbulent microstructure. *J. Atmos. Oceanic Tech.* **12**: 367-380.

Seim, H., 1999. Acoustic backscatter from salinity microstructure. *J. Atmos. Oceanic Tech.* **16**: 1491-1498.

Sandstrom, H., J. Elliott, and N. Cochrane, 1989. Observing groups of solitary internal waves and turbulence with BATFISH and echo-sounder, *J. Phys. Oceanogr.* **19**: 987-997.

Stanton, T. K., 1989. Simple approximate formulas for backscattering of sound by spherical and elongated objects, *J. Acoust. Soc. Am.* **86**(4): 1499-1510.

Stanton, T. K., D. Chu, P. Wiebe, and C. Clay, 1993. Average echoes from randomly oriented random-length finite cylinders: Simple physics and application to zooplankton, *J. Acoust. Soc. Am.* **94**: 3463-3472.

Stanton, T. K., P. Wiebe, D. Chu, and L. Goodman, 1994a. Acoustic characterization and discrimination of marine zooplankton and turbulence, *ICES J. Mar. Sci.* **51**: 469-479.

Stanton, T., Wiebe, P., Chu, D., Benfield, M., Scanlon, L., Martin, L., and Eastwood, R., 1994b. On acoustic estimates of zooplankton biomass. *ICES J. Mar. Sci.* **51**: 505-512.

Stanton, T. K., and D. Chu, 2000. Review and recommendations for the modeling of acoustic scattering by fluid-like elongated zooplankton: euphausiids and copepods, *ICES J. Mar. Sci.* **57**: 793-807.

Trevorrow, M., and Y. Tanaka, 1997. Acoustic and in situ measurements of freshwater amphipods (*Jesogammarus annandalei*) in Lake Biwa, Japan, *Limnol. Oceanogr.* **42**(1): 121-132.

Trevorrow, M., 1998. Observations of internal solitary waves near the Oregon coast with an inverted echo-sounder, *J. Geophys. Res.* **103**(C4): 7671-7680.

Warren, J., 2000. Estimating Gulf of Maine zooplankton distributions using multiple frequency acoustic, video and environmental data. PhD dissertation Dept. of Ocean Engineering, MIT and Wood's Hole Oceanographic Institution.

Wiebe, P, C. Greene, T. Stanton, and J. Burczynski, 1990. Sound scattering by live zooplankton and micronekton: empirical studies with a dual beam acoustic system, *J. Acoust. Soc. Am.* **88**(5): 2346-2360.

Wesson, J., and M. Gregg, 1994. Mixing at Carmainal Sill in the Strait of Gibraltar, *J. Geophys. Res.* **99**: 9847-9878.

Appendix 1: Crustacean Zooplankton Scattering Models

Detailed modeling and measurement of zooplankton scattering is a messy business, and has been pursued by only a few investigators (e.g. Johnson 1977; Kristensen & Dahlen 1986; Greene et al. 1989; Stanton 1989; Wiebe et al. 1990). At present there is no universally applicable scattering model. Current literature has focused almost exclusively on euphausiids and copepods, as these species are the most generally abundant throughout the world's ocean. The modeling approach approximates the zooplankter as an idealized shape of fluid-like material having a small contrast in density and sound speed relative to seawater. Usual modeling approximations are spherical or cylindrical, with the characteristic dimension usually taken as the equivalent spherical radius, *esr*. Purely empirical approaches are also employed, generally fitting a curve of the form $TS = A + B \cdot \log[\text{frequency}]$, where *TS* is target strength (=10·log[back-scatter cross-section] and A, B are constants. Overall, the acoustic scattering can be divided into two regimes: 1) the *Rayleigh* regime at relatively low frequencies where the scattering cross-section increases as approximately the fourth-power of the acoustic wave-number (or frequency), and 2) a higher-frequency *geometric* regime where there is a weaker or no frequency dependence. The transition region between these regimes lies near $k \cdot esr \approx 1$. In the Rayleigh regime the particular choice of scattering model is less important, so a spherical approximation is usual. Through the transition region into the geometric regime, the choice of scattering model becomes important as the effects of zooplankter elongation, curvature, and orientation become more important. For example, Trevorrow & Tanaka (1997) found that a cylindrical model for 9 mm long amphipods better fit the measured scattering strengths in the 50 to 200 kHz transition region. Stanton & Chu (2000) present an overview of the various modeling approaches and their applicability. Given uncertainties in species, size, orientation, and the fact that echo-sounder measurements are samples over many individuals, it seems reasonable to use only simple, approximate formulae.

Figures A1 and A2 show comparisons of modeling and measurements for the two dominant classes of zooplankton found in B.C. coastal waters. The various simplified scattering models are taken from Stanton (1989), with scattering data from Greenlaw (1977) and Stanton et al. (1993). Specifically, the backscatter cross-section for a single zooplankter of radius a (*esr* or cylindrical equivalent), length L, and radius of curvature ρ (for the bent cylinder), at wavenumber k, is given by

$$\sigma_{bs}(a,L,k) = \begin{cases} \dfrac{a^2 (ka)^4 \alpha_s^2 G}{1+[4(ka)^4 \alpha_s^2]/(R^2 F)} & \textit{sphere} \\ \dfrac{\frac{1}{4} L^2 (ka)^4 \alpha_c^2 G}{1+[\pi (ka)^3 \alpha_c^2]/(R^2 F)} & \textit{cylinder} \\ \dfrac{\frac{1}{4} L^2 (ka)^4 \alpha_c^2 H^2 G}{1+[L^2 (ka)^4 \alpha_c^2 H^2]/(\rho a R^2 F)} & \textit{bent cylinder} \end{cases}$$

where

$$\alpha_s = \frac{1-gh^2}{3gh^2} + \frac{1-g}{1+2g}, \qquad \alpha_c = \frac{1-gh^2}{2gh^2} + \frac{1-g}{1+g}, \qquad R = \frac{gh-1}{gh+1}$$

with g = density ratio (= 1.045) and h = sound speed ratio (= 1.025) of the zooplankter body with respect to seawater. For the cylinder and bent cylinder models these expressions are for broadside incidence. The functions F, G, and H are selected to modify the basic expressions for euphausiids to reproduce resonant nulls and geometric regime dependencies observed in the data, specifically

	Sphere	*Cylinders*
F	$7(ka)^{-0.2}$	$2(ka)^{-1}$
G	$1-0.7\exp[-2.5(ka-2.5)^2]$	$1-0.8\exp[-2(ka-1.2)^2]$

and for the bent cylinder case, $H = \frac{1}{2} + \frac{1}{2}(\rho/L)\sin(L/\rho)$. For euphausiids an empirical relation $esr = 0.136 \cdot L^{1.05}$ should be used, whereas for copepods a relation $esr = 0.25 \cdot L$ is applicable. The empirical relation for euphausiids due to Kristensen & Dahlen (1986) takes a form similar to the spherical model, with an added damped resonant peak, i.e.

$$\sigma_{bs} = \frac{\alpha_s^2 a^2}{\left[(f_0/f)^2 - 1\right]^2 + d^2}, \text{ with } f_0 \text{ evaluated at } k \cdot a = 1.2 \text{ and } d = 0.8.$$

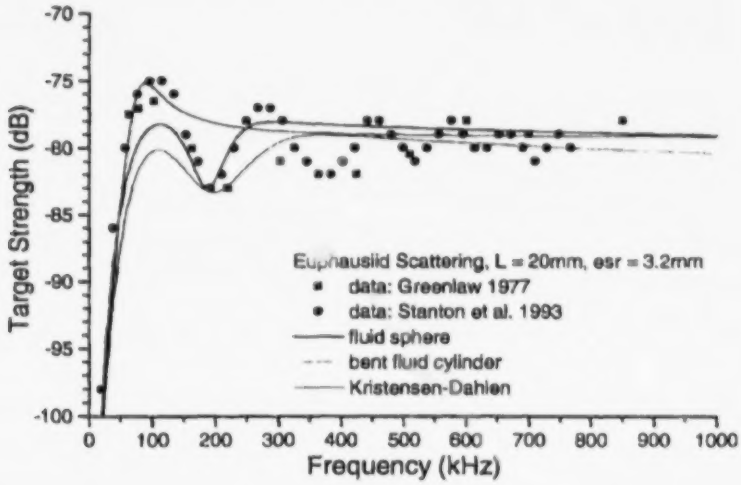

Figure A1: Comparison of Euphausiid acoustic scattering models for length = 20mm.

For the euphausiid case (Fig. A1), the fluid sphere and bent cylinder models have been empirically modified to reproduce the null near 200 kHz, which is due to a mechanical resonance near $k \cdot esr \approx 2$ and is clearly indicated in the scattering data. For the euphausiid case the modified fluid sphere model provides the best fit over the entire frequency range, while the empirical model due to Kristensen & Dahlen (1986) provides the best fit to the data at frequencies below 120 kHz. In the case of copepods the simple fluid cylinder model appears to be the best fit to the data over a wide range of frequencies. Overall, for the usual echo-sounder frequencies (in the range 38 to 200 kHz), euphausiids lie in the transition region while copepods lie in the Rayleigh regime. This suggests that, in the absence of other confounding zooplankton or microstructure scattering, the use of two or more medium

frequency echo-sounders should enable quantitative discrimination between euphausiids and copepods.

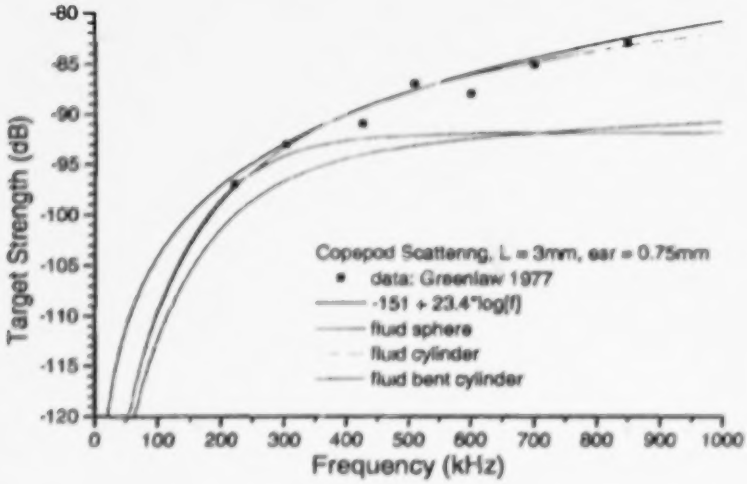

Figure A2: Comparison of Copepod acoustic scattering models.

Appendix 2: Acoustic Scattering from Turbulent Microstructure

This section is summarized from models presented by Seim et al. (1995) and Seim (1999), used by Sandstrom et al. (1989) and Trevorrow (1998), and as described by Warren (2000). In this Knight Inlet region the near-surface stratification is induced by both temperature and salinity gradients, thus a microstructure scattering theory including both components should be used. Fluctuations in both temperature and salinity induce changes in the effective index of refraction of seawater, which can be related to the acoustic backscatter cross-section through a Bragg scattering mechanism. Including turbulence models for both the inertial-convective and viscous-convective regimes the acoustic backscattering can be related to the turbulent kinetic energy dissipation rate, ε ($W \cdot kg^{-1}$), the temperature variance dissipation rate, χ_T ($°C^2 \cdot s^{-1}$), and bulk properties of the fluid such as temperature and salinity gradients and the buoyancy frequency. Hence, the acoustic back-scattering cross-section per unit volume, assuming isotropic turbulence and no correlation between temperature and salinity fluctuations, is given by

$$\sigma_{bs} = \begin{cases} A \cdot \frac{1}{96} \cdot \chi_T \cdot \left(\frac{k_{Br}}{\varepsilon}\right)^{\frac{1}{3}} \left(b_T^2 + \frac{b_S^2}{\delta^2}\right) & for\ k < k_* \\ q\left(\frac{\nu}{\varepsilon}\right)^{\frac{1}{2}} \left(\frac{\chi_T \cdot k_{Br}}{32}\right) \left[b_T^2 \exp(-\tfrac{1}{2}\beta_T^2) + \frac{b_S^2}{\delta^2} \exp\left(-\tfrac{1}{2}\beta_S^2\right)\right] & for\ k > k_* \end{cases}$$

where the boundary between inertial-convective and viscous-convective regimes lies at a critical wavenumber $k_* = (\varepsilon/\nu)^{\frac{1}{4}} / 8$ and the constant A is chosen to match the two spectra at $k = k_*$. In these relations $q = 3.7$, ν is kinematic viscosity of seawater (1×10^{-6} m^2 s^{-1}), k_{Br} is the backscatter Bragg wavenumber ($= 4\pi f / c$ where f is acoustic frequency and c is sound speed), b_T is the sound speed sensitivity to temperature [$c^{-1}(\partial c/\partial T)$], b_S is the sound speed sensitivity to salinity [$c^{-1}(\partial S/\partial T)$], δ is the ratio of vertical temperature and salinity gradients [$(\partial T/\partial z)\cdot(\partial S/\partial z)^{-1}$], with

$$\beta_T = \sqrt{2q} \cdot k_{Br} \cdot \left(\nu \cdot D_T^2 \cdot \varepsilon^{-1}\right)^{0.25} \text{ and } \beta_S = \sqrt{2q} \cdot k_{Br} \cdot \left(\nu \cdot D_S^2 \cdot \varepsilon^{-1}\right)^{0.25},$$

where D_T and D_S are the molecular diffusivities due to heat and salt (respectively 1.4×10^{-7} m^2 s^{-1} and 1.4×10^{-9} m^2 s^{-1}), and finally χ_T is given approximately by

$$\chi_T \approx 0.4 \cdot \varepsilon \cdot N^{-2} (\partial T/\partial z)^2,$$

where N is the buoyancy frequency (s^{-1}). For typical seawater water conditions the values of b_T and b_S are 2.5×10^{-3} $°C^{-1}$ and 8.2×10^{-4} psu^{-1}, respectively. Figure A3 shows an evaluation of these models for typical Knight Inlet conditions. At frequencies in the 100 to 500 kHz range these microstructure scattering spectra have a similar level and shape to the zooplankton spectra, making it difficult to distinguish between the two on the basis of scattering strength alone. However, at lower frequencies (<50kHz) the turbulence scattering stays relatively strong. In this situation the value of δ is –0.2 and thus the ratio of temperature to salinity contributions to the refractive index fluctuations is roughly -0.6. Clearly the salinity contributions are significant, especially at higher frequencies where thermal diffusivity effects

reduces the temperature contributions, i.e. at wavenumbers above $k_T = (\varepsilon/\nu D_T^2)^{\frac{1}{4}}$. Because the molecular diffusivity of salt is two orders of magnitude smaller, the salinity contributions extend to much higher wavenumbers and frequencies.

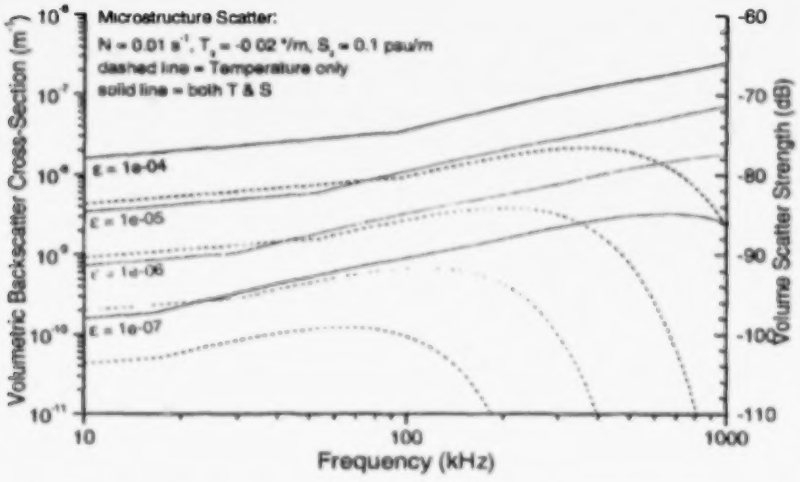

Figure A3 Acoustic backscatter strength vs. frequency due to microstructure scattering for typical Knight Inlet conditions and turbulent dissipation rates from 10^{-7} to 10^{-4} W·kg^{-1}. Dashed lines correspond to temperature contributions only, while solid lines include both temperature and salinity contributions.

UNCLASSIFIED
SECURITY CLASSIFICATION OF FORM
(highest classification of Title, Abstract, Keywords)

DOCUMENT CONTROL DATA

(Security classification of title, body of abstract and indexing annotation must be entered when the overall document is classified)

1. ORIGINATOR (the name and address of the organization preparing the document. Organizations for whom the document was prepared, e.g. Establishment sponsoring a contractor's report, or tasking agency, are entered in section 8.)

Defence Research Establishment Atlantic
PO Box 1012
Dartmouth, Nova Scotia, Canada B2Y 3Z7

2. SECURITY CLASSIFICATION (overall security classification of the document including special warning terms if applicable).

UNCLASSIFIED

3. TITLE (the complete document title as indicated on the title page. Its classification should be indicated by the appropriate abbreviation (S,C,R or U) in parentheses after the title)

Zooplankton aggregations near a coastal sill: an examination of echo-sounder data from August and September 1995 in Knight Inlet, B.C. (U)

4. AUTHORS (Last name, first name, middle initial. If military, show rank, e.g. Doe, Maj. John E.)

Trevorrow, Mark V.

5. DATE OF PUBLICATION (month and year of publication of document)	6a. NO. OF PAGES (total containing information. Include Annexes, Appendices, etc)	6b. NO. OF REFS (total cited in document)
September 2001	37	25

7. DESCRIPTIVE NOTES (the category of the document, e.g. technical report, technical note or memorandum. If appropriate, enter the type of report, e.g. interim, progress, summary, annual or final. Give the inclusive dates when a specific reporting period is covered)

TECHNICAL MEMORANDUM

8. SPONSORING ACTIVITY (the name of the department project office or laboratory sponsoring the research and development. Include address).

Defence Research Establishment Atlantic

9a. PROJECT OR GRANT NO. (if appropriate, the applicable research and development project or grant number under which the document was written. Please specify whether project or grant)	9b. CONTRACT NO. (if appropriate, the applicable number under which the document was written)
1DA	US Office of Naval Research N00014-01-1-0273

10a. ORIGINATOR'S DOCUMENT NUMBER (the official document number by which the document is identified by the originating activity. This number must be unique to this document.)	10b. OTHER DOCUMENT NOs. (Any other numbers which may be assigned this document either by the originator or by the sponsor.)
DREA TM 2001-119	

11. DOCUMENT AVAILABILITY (any limitations on further dissemination of the document, other than those imposed by security classification)

(✔) Unlimited distribution
( ) Defence departments and defence contractors; further distribution only as approved
( ) Defence departments and Canadian defence contractors; further distribution only as approved
( ) Government departments and agencies; further distribution only as approved
( ) Defence departments; further distribution only as approved
( ) Other (please specify):

12. DOCUMENT ANNOUNCEMENT (any limitation to the bibliographic announcement of this document. This will normally correspond to the Document Availability (11). However, where further distribution (beyond the audience specified in (11)) is possible, a wider announcement audience may be selected).

UNCLASSIFIED
SECURITY CLASSIFICATION OF FORM
(highest classification of Title, Abstract, Keywords)

13. ABSTRACT (a brief and factual summary of the document. It may also appear elsewhere in the body of the document itself. It is highly desirable that the abstract of classified documents be unclassified. Each paragraph of the abstract shall begin with an indication of the security classification of the information in the paragraph (unless the document itself is unclassified) represented as (S), (C), (R), or (U). It is not necessary to include here abstracts in both official languages unless the text is bilingual)

(U) This report presents a retrospective study of echo-sounder and other physical oceanographic data collected in Knight Inlet, British Columbia during the late summer of 1995. This present study was undertaken to provide oceanographic background and assist planning for focused field experiments on zooplankton aggregations which will be conducted in this same area in the autumn of 2001. High-frequency (120 and 200 kHz, uncalibrated) echo-sounder data from two separate vessels is examined under both ebb and flood tide conditions, and for diurnal variations. The 1995 data revealed dramatic tidally-driven internal hydraulic flows over-top of a 65 m deep sill in Knight Inlet, created by strong, near-surface (<20 m depth) thermohaline stratification. In general the zooplankton populations exhibited classic diurnal migration habits, forming into relatively dense layers at 70 to 120 m depth during daytime and dispersing throughout the entire water column at night. This behavior is suggestive that the zooplankton scattering layers were dominated by Euphausiids, which are common in B.C. coastal inlets. During daytime on both ebb and flood tides there was evidence that the zooplankton layers were trapped and concentrated by the flow against the upstream side of the sill. A comparison of acoustic scattering with *in situ* temperature, salinity, and turbulence profiles suggests that microstructure scattering is responsible for distinct *flow lines* appearing in the strongly stratified near-surface region, however zooplankton scattering is found to dominate at greater depths. For the autumn 2001 field experiments, behavioral hypotheses and recommendations are given for using calibrated, multi-frequency echo-sounders in conjunction with net trawls and *in situ* optical sampling techniques.

14. KEYWORDS, DESCRIPTORS or IDENTIFIERS (technically meaningful terms or short phrases that characterize a document and could be helpful in cataloguing the document. They should be selected so that no security classification is required. Identifiers, such as equipment model designation, trade name, military project code name, geographic location may also be included. If possible keywords should be selected from a published thesaurus, e.g. Thesaurus of Engineering and Scientific Terms (TEST) and that thesaurus identified. If it is not possible to select indexing terms which are Unclassified, the classification of each should be indicated as with the title)

zooplankton, high-frequency echo-sounder, turbulent microstructure

Defence R&D Canada
is the national authority for providing
Science and Technology (S&T) leadership
in the advancement and maintenance
of Canada's defence capabilities.

R et D pour la défense Canada
est responsable, au niveau national, pour
les sciences et la technologie (S et T)
au service de l'avancement et du maintien des
capacités de défense du Canada.

#516524

CA011952

DEFENCE R&D DÉFENSE

www.drdc-rddc.dnd.ca